The Plant Cell, Vol. 24: 2898–2916, July 2012, www.plantcell.org

The *Arabidopsis* Mediator Subunit MED25 Differentially Regulates Jasmonate and Abscisic Acid Signaling through Interacting with the MYC2 and ABI5 Transcription Factors [C][W][OA]

Rong Chen,[1] Hongling Jiang,[1] Lin Li, Qingzhe Zhai, Linlin Qi, Wenkun Zhou, Xiaoqiang Liu, Hongmei Li,[2] Wenguang Zheng,[3] Jiaqiang Sun, and Chuanyou Li[4]

State Key Laboratory of Plant Genomics, National Centre for Plant Gene Research (Beijing), Institute of Genetics and Developmental Biology, Chinese Academy of Sciences, Beijing 100101, China

Transcriptional regulation plays a central role in plant hormone signaling. At the core of transcriptional regulation is the Mediator, an evolutionarily conserved, multisubunit complex that serves as a bridge between gene-specific transcription factors and the RNA polymerase machinery to regulate transcription. Here, we report the action mechanisms of the MEDIATOR25 (MED25) subunit of the *Arabidopsis thaliana* Mediator in regulating jasmonate- and abscisic acid (ABA)–triggered gene transcription. We show that during jasmonate signaling, MED25 physically associates with the basic helix-loop-helix transcription factor MYC2 in promoter regions of MYC2 target genes and exerts a positive effect on MYC2-regulated gene transcription. We also show that MED25 physically associates with the basic Leu zipper transcription factor ABA-INSENSITIVE5 (ABI5) in promoter regions of ABI5 target genes and shows a negative effect on ABI5-regulated gene transcription. Our results reveal that underlying the distinct effects of MED25 on jasmonate and ABA signaling, the interaction mechanisms of MED25 with MYC2 and ABI5 are different. These results highlight that the MED25 subunit of the *Arabidopsis* Mediator regulates a wide range of signaling pathways through selectively interacting with specific transcription factors.

INTRODUCTION

The jasmonate family of oxylipins, including jasmonic acid (JA) and its bioactive derivatives, which are collectively referred to as JAs, regulates diverse aspects of plant immunity and development. It is generally believed that, in addition to promoting plant defense responses to herbivore attack, pathogen infection, and mechanical wounding, JAs also inhibit growth-related processes such as cell division and photosynthesis (Creelman and Mullet, 1997; Turner et al., 2002; Browse, 2005, 2009; Wasternack, 2007; Howe and Jander, 2008; Kazan and Manners, 2008; Chung et al., 2009; Pauwels et al., 2009; Sun et al., 2011). Underlying these important physiological effects, JAs orchestrate genome-wide transcriptional reprogramming of plant cells to coordinate growth- and defense-related processes.

Much of our understanding of the JA signal transduction pathway has come from the recent elucidation of the molecular details of JA-regulated gene transcription. Conventional genetic evidence together with recent biochemical and structural studies support the view that the F-box protein CORONATINE INSENSITIVE1 (COI1) is the receptor of jasmonoyl-L-Ile (JA-Ile), a molecularly active form of JA (Xie et al., 1998; Katsir et al., 2008; Fonseca et al., 2009; Yan et al., 2009; Sheard et al., 2010; Suza et al., 2010; Wasternack and Kombrink, 2010). Significant advancement in our understanding of how the JA signaling operates came from the discovery that the JASMONATE ZIM DOMAIN (JAZ) proteins, which serve as transcriptional repressors of JA-induced gene expression, are substrates of the E3 ubiquitin ligase SCF^{COI1} (Chini et al., 2007; Thines et al., 2007; Yan et al., 2007; Chung et al., 2009). Recent structure-function studies indicated that the jasmonate receptor is a three-molecule complex consisting of COI1, JAZ transcriptional repressors, and inositol pentakisphosphate (Sheard et al., 2010). These studies together revealed that jasmonate and auxin show a similar signal perception and transduction paradigm, in which F-box proteins (receptors) mediate the degradation of negative regulators of gene transcription cascades (Mockaitis and Estelle, 2008). At low JA levels, JAZ proteins interact with NOVEL INTERACTOR OF JAZ (NINJA) to recruit TOPLESS (TPL) as a corepressor to repress the activity of JAZ-targeted transcription factors, including the basic helix-loop-helix (bHLH) transcription factor MYC2, which regulates diverse aspects of JA-mediated gene expression (Boter et al., 2004; Lorenzo et al., 2004; Dombrecht et al., 2007; Pauwels et al., 2010). In response to internal or external cues, JA-Ile is quickly synthesized by JASMONATE RESISTANT1 (JAR1) (Staswick and Tiryaki, 2004; Fonseca et al.,

[1] These authors contributed equally to this work.
[2] Current address: Photosynthesis Research Center, Key Laboratory of Photobiology, Institute of Botany, Chinese Academy of Sciences, Nanxincun 20, Xiangshan, Beijing 100093, China.
[3] Current address: Department of Biology, Saint Louis University, 3507 Laclede Ave., St. Louis, MO 63103.
[4] Address correspondence to cyli@genetics.ac.cn.
The author responsible for distribution of materials integral to the findings presented in this article in accordance with the policy described in the Instructions for Authors (www.plantcell.org) is: Chuanyou Li (cyli@genetics.ac.cn).
[C] Some figures in this article are displayed in color online but in black and white in the print edition.
[W] Online version contains Web-only data.
[OA] Open Access articles can be viewed online without a subscription.
www.plantcell.org/cgi/doi/10.1105/tpc.112.098277

2009; Suza et al., 2010; Wasternack and Kombrink, 2010). JA-Ile then acts as "molecular glue" to stimulate the interaction of its coreceptors COI1 and JAZs and, as a consequence, promotes the degradation of the JAZ repressors. Degradation of JAZ proteins leads to the liberation of MYC2 from NINJA and TPL and initiates the transcriptional reprogramming of the cells and the activation of the JA responses (Chini et al., 2007; Thines et al., 2007; Pauwels et al., 2010; Sheard et al., 2010). In addition to MYC2, several other transcription factors targeted by JAZs were recently identified. Among them, MYC3 and MYC4 act additively with MYC2 in the regulation of root growth inhibition and defense responses (Fernández-Calvo et al., 2011). The WD-repeat/bHLH/MYB transcription factor complexes TRANSPARENT TESTA8/GLABRA3 (GL3)/ENHANCER OF GL3/MYB75/GL1 are involved in JA-induced anthocyanin accumulation and trichome initiation (Qi et al., 2011). The R2R3-MYB transcription factors MYB21/MYB24 are specifically involved in JA-dependent anther development (Song et al., 2011).

Emerging evidence has revealed the involvement of the Mediator complex in JA-induced transcriptional regulation (Kidd et al., 2009). Mediator is a conserved multisubunit complex known to promote the transcription of protein-coding genes by RNA polymerase II (Pol II) in eukaryotes. Mediator was first identified from yeast as required for activator-dependent stimulation of Pol II transcription (Kelleher et al., 1990; Flanagan et al., 1991). Later it was shown that the yeast Mediator is a multiprotein complex that forms three submodules, the head, middle, and tail, with the head submodule serving as the Pol II–interacting interface and the tail submodule interacting with sequence-specific transcription factors (Chadick and Asturias, 2005). It was now realized that Mediator is highly conserved in a wide range of eukaryotes, including mammals and plants (Chadick and Asturias, 2005; Malik and Roeder, 2005; Bäckström et al., 2007). The studies over the last decade reveal that, besides interacting directly with Pol II, Mediator has multiple functions and can interact with and coordinate the action of numerous other coactivators and corepressors, including those acting at the level of chromatin (Kidd et al., 2010, 2011; Malik and Roeder, 2010; Borggrefe and Yue, 2011; Chen and Roeder, 2011; Conaway and Conaway, 2011; Hentges, 2011; Kim and Chen, 2011; Ries and Meisterernst, 2011).

The recent purification of the *Arabidopsis thaliana* Mediator complex identified 21 conserved and six plant-specific subunits (Bäckström et al., 2007). Among the few genetically characterized *Arabidopsis* Mediator subunits (Autran et al., 2002; Wang and Chen, 2004; Gillmor et al., 2010; Ito et al., 2011; Kidd et al., 2011; Kim et al., 2011), MEDIATOR25 (MED25) was shown to play multiple roles in regulating flowering (Cerdán and Chory, 2003), organ size (Xu and Li, 2011), stress responses (Elfving et al., 2011), and, notably, JA signaling (Kidd et al., 2009). These studies suggest that a single Mediator subunit can serve as the interface for several diverse transcriptional regulators and raise a significant question of how a high degree of plasticity of a single Mediator subunit is achieved.

Here, we investigate the distinct action mechanisms of MED25 in regulating JA- and abscisic acid (ABA)–induced gene expression. We show that MED25 interacts with the bHLH transcription factor MYC2 and executes a positive effect on MYC2-regulated expression of JA-responsive genes. We also show that MED25 interacts with the basic domain/Leu zipper (bZIP) transcription factor ABA-INSENSITIVE5 (ABI5) and exerts a negative effect on ABI5-regulated expression of ABA-responsive genes. We provide evidence showing that the conserved activator-interacting domain (ACID) of MED25 is sufficient for its interaction with ABI5 but not sufficient for its interaction with MYC2. In addition, we reveal that while the putative transcriptional activation domain (TAD) of MYC2 is involved in its interaction with MED25, the TAD domain of ABI5 is not involved in its interaction with MED25. These findings highlight that, in response to different hormonal signals, a single plant Mediator subunit can regulate distinct transcriptional programs via interactions with relevant gene-specific transcription factors.

RESULTS

The *ber6* Mutant Contains a Mutation in the *MED25* Gene and Affects Diverse Aspects of JA Responses

The *bestatin-resistant6* (*ber6*) line of *Arabidopsis* was identified as a JA-insensitive mutant in JA-induced root growth inhibition (Zheng et al., 2006). Our further characterization of *ber6* was performed with a homozygous line obtained from five successive backcrosses of the original mutant to the wild type Columbia-0 (Col-0). JA response assays with this line showed that *ber6* was generally less sensitive than the wild type to the inhibition effect of a range of concentrations of JA on root growth (Figure 1A). We then examined whether the expression of JA-responsive genes is affected in *ber6* plants. Two distinct branches of JA-responsive genes that are differentially regulated by the transcription factor MYC2 were identified in *Arabidopsis* (Boter et al., 2004; Lorenzo et al., 2004). One of these branches, including the *VEGETATIVE STORAGE PROTEIN1* (*VSP1*) gene (Berger et al., 1995), is believed to be involved in plant responses to wounding. The other branch, including the plant defensin gene *PDF1.2* (Penninckx et al., 1996), is considered to be associated with plant responses to pathogen infection (Boter et al., 2004; Lorenzo et al., 2004). Promoter-reporter fusion assays revealed that the *ber6* mutation substantially impaired JA-induced expression of both $VSP1_{pro}$:*GUS* (for β-glucuronidase) and $PDF1.2_{pro}$:*LUC* (for luciferase) (Figures 1B and 1C). Consistent with this, quantitative real-time PCR (qRT-PCR) assays showed that the JA-induced expression levels of *VSP1* (Figure 1D) and *PDF1.2* (Figure 1E) were markedly reduced in *ber6* compared with those in the wild type. Next, we examined the response of *ber6* plants to infection by *Pseudomonas syringae* pv *tomato* (*Pst*) DC3000. As measured by leaf symptoms (Figure 1F) and pathogen growth (Figure 1G) of the infected plants, the effects of *Pst* DC3000 infection in *ber6* are largely similar to those in the *coi1-2* mutant, which harbors a point mutation of the JA receptor gene *COI1* and therefore is resistant to *Pst* DC3000 (Kloek et al., 2001; Xu et al., 2002; Laurie-Berry et al., 2006). Together, our results support that *ber6* is a JA signaling mutant that is defective in JA-induced defense gene expression.

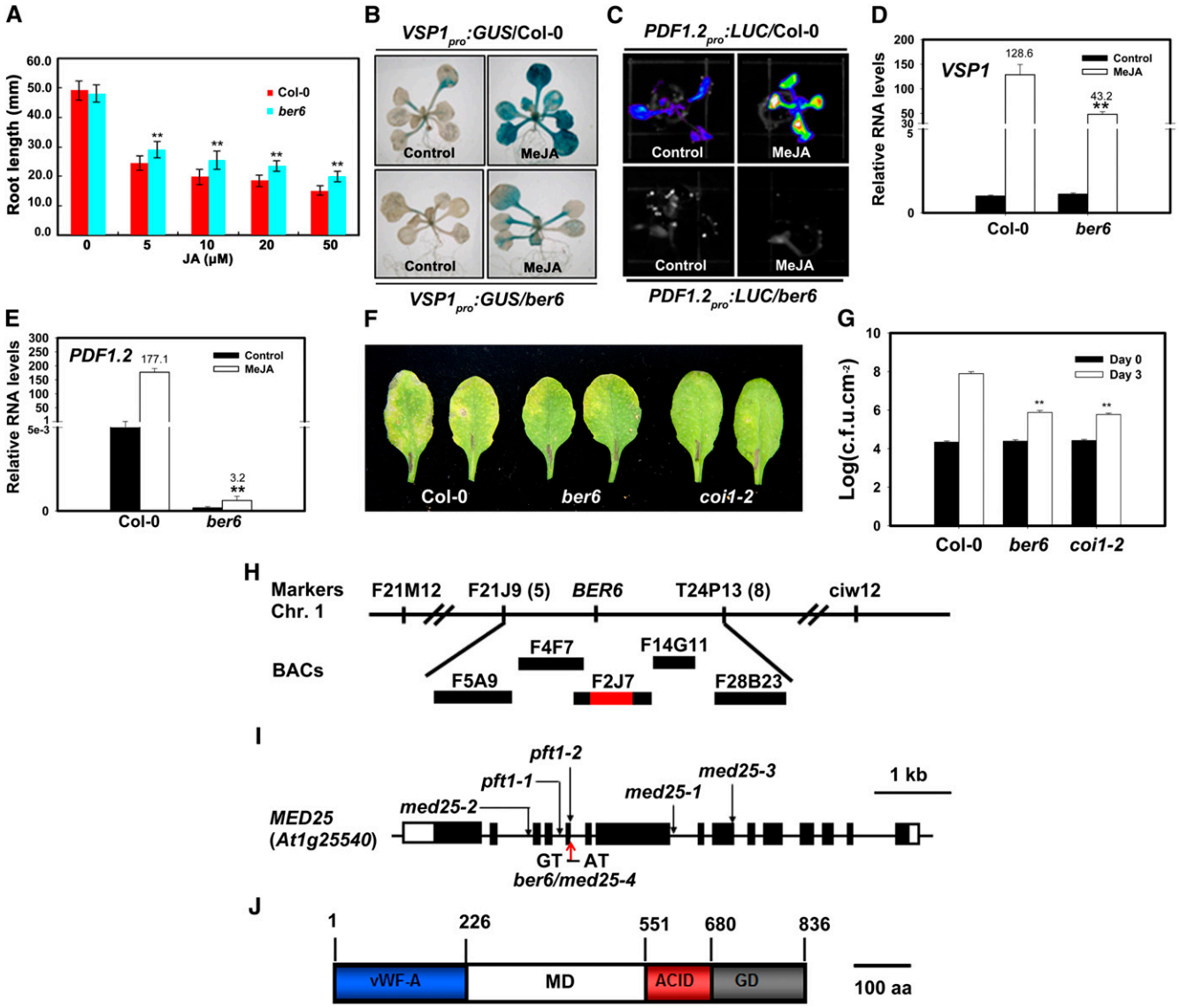

Figure 1. The Defective JA Responses of the *ber6* Mutant Are Caused by a Mutation of the *MED25* Gene.

(A) Root growth inhibition assay of 10-d-old seedlings from Col-0 and *ber6* grown in MS medium containing indicated concentrations of JA. Results shown are the mean ± SD of measurements from 90 seedlings. For each JA concentration, the data were analyzed by Student's *t* test using SPSS. Asterisks denote *t* test significance compared with JA-grown wild type plants: **P < 0.01.

(B) Photographs of representative control and 50 μM MeJA (6-h treatments) treated 10-d-old seedlings of *VSP1*$_{pro}$:*GUS*/Col-0 and *VSP1*$_{pro}$:*GUS*/*ber6*.

(C) Photographs of representative control and 50 μM MeJA (48-h treatments) treated 10-d-old seedlings of *PDF1.2*$_{pro}$:*LUC*/Col-0 and *PDF1.2*$_{pro}$:*LUC*/*ber6*.

(D) and **(E)** qRT-PCR analysis of *VSP1* (6-h treatments; **[D]**) and *PDF1.2* (48-h treatments; **[E]**) RNA levels in 10-d-old Col-0 and *ber6* seedlings treated with 50 μM MeJA. The break ranges are shown on the *y* axis. Data shown are mean values of three biological repeats with SD. Asterisks denote Student's *t* test significance compared with MeJA-treated Col-0 plants: **P < 0.01. Numbers on the white bars represent fold induction values in MeJA-treated plants relative to control (black bars) plants.

(F) Symptoms on rosette leaves of 4-week-old soil-grown Col-0, *ber6*, and *coi1-2* following inoculation with *Pst* DC3000 bacteria for 3 d.

(G) *Pst DC3000* populations, shown as colony-forming units (c.f.u.) cm^{-2} of leaf area in Col-0, *ber6*, and *coi1-2* plants at day 0 (black) and day 3 (white) after inoculation. Asterisks denote Student's *t* test significance compared with *Pst* DC3000–treated Col-0 plants: **P < 0.01.

(H) Fine genetic and physical mapping of *BER6*. The target gene was mapped to a genetic interval between markers F21J9 and T24P13 on chromosome 1. Analysis of a F2 mapping population of 1800 plants delimited the gene to a region of 50 kb on the BAC clone F2J7 (red). Numbers in parentheses indicate the number of recombination events identified between markers and the target gene.

(I) *MED25* gene structure, showing the mutation site of *ber6*/*med25-4*. The T-DNA insertion sites in *med25-2*, *med25-3*, *pft1-1*, and *pft1-2* and the point mutation site of *med25-1* are also indicated. Black boxes represent exons, lines represent introns, and white boxes represent 5′(3′)-untranslated region, respectively. Bar = 1 kb.

(J) Schematic representation of MED25 protein. The MED25 protein contains a vWF-A domain (blue), an MD domain (white), an ACID domain (red), and a GD domain (gray). Bar = 100 amino acids (aa).

The decreased JA-induced root growth inhibition of *ber6* provides a facile assay for map-based cloning studies aimed at determining the genetic basis of this defect. Using a total of 1800 F2 plants showing the mutant phenotype, *BER6* was delimited to a 50-kb region on the BAC clone F2J7 (Figure 1H). DNA sequencing revealed that *ber6* contains a G-to-A transition at the junction between the fifth exon and the fifth intron of the annotated gene At1g25540 (Figure 1I), which encodes the MED25 subunit of the *Arabidopsis* Mediator (Bäckström et al., 2007). The G-to-A mutation in *ber6* destroys an *Rsa*I restriction site, and a cleaved amplified polymorphic sequence marker was developed to detect the *ber6* mutant allele (see Supplemental Figure 1C online). In the *ber6* mutant, the 5′ exon-intron boundary of intron 5 is changed from GT to AT (Figure 1I), replacing a G that is highly conserved at plant gene splice sites. The mutation in *ber6* altered the splicing of At1g25540 mRNA (see Supplemental Figure 1A online), resulting in a frame shift that destroys the von Willebrand Factor A (vWF-A) domain, which has been shown to be crucial for the binding of MED25 to the Mediator complex (Mittler et al., 2003). Protein gel analysis using anti-MED25 antibodies failed to detect MED25 protein accumulation in the *ber6* mutant (see Supplemental Figure 1B online). For genetic complementation of the *ber6* phenotype, the *MED25* cDNA from the wild type was introduced into *ber6* mutants under the control of the 35S promoter of *Cauliflower mosaic virus*. The results showed that the *MED25* cDNA complemented the *ber6* mutant in JA-mediated root growth inhibition (see Supplemental Figure 1C online). These results support that the defective JA response phenotype of *ber6* is resulted from the identified G-to-A mutation of *MED25*. Since several mutant alleles of the *MED25* gene have been described (Cerdán and Chory, 2003; Xu and Li, 2011), we henceforth designated the *ber6* allele as *med25-4*. Further confirmation that *BER6* encodes MED25 came from analyses of several reported mutant alleles of *MED25* (Figure 1I). *pft1-1*, the original mutant allele of *MED25* (Cerdán and Chory, 2003), as well as the recently described alleles, including *pft1-2* (Kidd et al., 2009), *med25-1*, *med25-2*, and *med25-3* (Xu and Li, 2011), all displayed reduced sensitivity to JA in root growth inhibition (see Supplemental Figure 1E online). Genetic analyses showed that *ber6*/*med25-4* and *pft1-2* cannot complement each other in JA-induced root growth inhibition (see Supplemental Figure 1F online). In addition, *ber6*/*med25-4* displayed a late flowering phenotype when grown under long-day conditions (16 h light/8 h dark), as determined by rosette leaf number and bolting time (see Supplemental Figure 1G online). When grown under short-day conditions (10 h light/14 h dark), this mutant had similar rosette leaf number as the wild type but the bolting time showed a significant increase (see Supplemental Figure 1H online). Similar late flowering phenotype has also been observed in most of the reported mutant alleles of *MED25* (Cerdán and Chory, 2003; Kidd et al., 2009). Collectively, these results demonstrate that the *med25* mutation we identified is responsible for the *ber6* mutant phenotype.

The MED25 protein contains a vWF-A domain ($MED25^{1-226}$), a nonconserved middle domain (MD; $MED25^{227-550}$), an ACID domain ($MED25^{551-680}$), and a Gln-rich domain (GD; $MED25^{681-836}$) (Figure 1J). It is generally believed that the vWF-A domain is essential for the binding of MED25 to the Mediator complex, and the ACID domain is important for interaction with transcriptional activators, whereas the GD domain could be important for transcriptional activation (Cerdán and Chory, 2003; Mittler et al., 2003; Bäckström et al., 2007; Lee et al., 2007; Elfving et al., 2011).

MED25 Affects the Function of MYC2 in Regulating the Transcriptional Expression of JA-Responsive Genes

To elucidate the action mechanisms of MED25 in JA-mediated transcriptional regulation, we investigated the effect of MED25 on the function of MYC2, a master transcriptional regulator that controls diverse aspects of JA responses (Boter et al., 2004; Lorenzo et al., 2004; Dombrecht et al., 2007). Toward this goal, we generated a double mutant line *med25-4 myc2-2* and compared its JA responses with those of the single mutants in defense gene expression. Consistent with the well-recognized finding that MYC2 negatively regulates the expression of the branch of pathogen-responsive genes (Boter et al., 2004; Lorenzo et al., 2004; Dombrecht et al., 2007), our qRT-PCR assays indicated that JA-induced expression levels of *PDF1.2* (Figure 2A) and *ETHYLENE RESPONSE FACTOR1* (*ERF1*; Figure 2B) were markedly increased in *myc2-2* compared with those in the wild type. Importantly, JA-induced expression levels of these genes were strongly reduced in the *med25-4* mutant (Figures 1E, 2A, and 2B), suggesting that MED25 is required for JA-induced expression of this group of genes. Significantly, in the *med25-4 myc2-2* double mutant, JA-induced expression levels of *PDF1.2* and *ERF1* were essentially comparable to those in *med25-4* (i.e., *med25-4* suppressed the phenotype of *myc2-2* in terms of JA-induced *PDF1.2* and *ERF1* expression) (Figures 2A and 2B), suggesting that MED25 acts genetically downstream of MYC2 in regulating the expression of these genes. Together, these results support that, in response to JA, MED25 is required for the MYC2 function to repress the expression of pathogen-responsive genes. Consistent with the positive role of MYC2 in regulating the expression of wound-responsive genes (Boter et al., 2004; Lorenzo et al., 2004; Dombrecht et al., 2007), we found that the JA-induced expression levels of *VSP1* (Figure 2C), *LIPOXYGENASE2* (*LOX2*; Figure 2D), *JAZ6* (Figure 2E), and *JAZ8* (Figure 2F) were substantially reduced in *myc2-2* mutants compared with those in wild-type plants (Figures 2C to 2F). JA-induced expression levels of these genes were also reduced in *med25-4* (Figures 2C to 2F), suggesting that MED25 is also important for JA-induced expression of this group of genes. As expected, in the *med25-4 myc2-2* double mutant, JA-induced expression levels of these genes were largely similar to those in *med25-4* (Figures 2C to 2F), suggesting that MED25 is also important for the MYC2 function to activate the expression of these wound-responsive genes. Taken together, these results led us to the conclusion that, during JA response, MED25 exerts a positive effect on the function of the MYC2 transcription factor to regulate the expression of JA-responsive genes.

MED25 Is Recruited to Promoters of MYC2 Target Genes in a JA-Dependent Manner

It has been shown that the human MED25, together with the retinoic acid (RA)–bound retinoic acid receptor (RAR), was

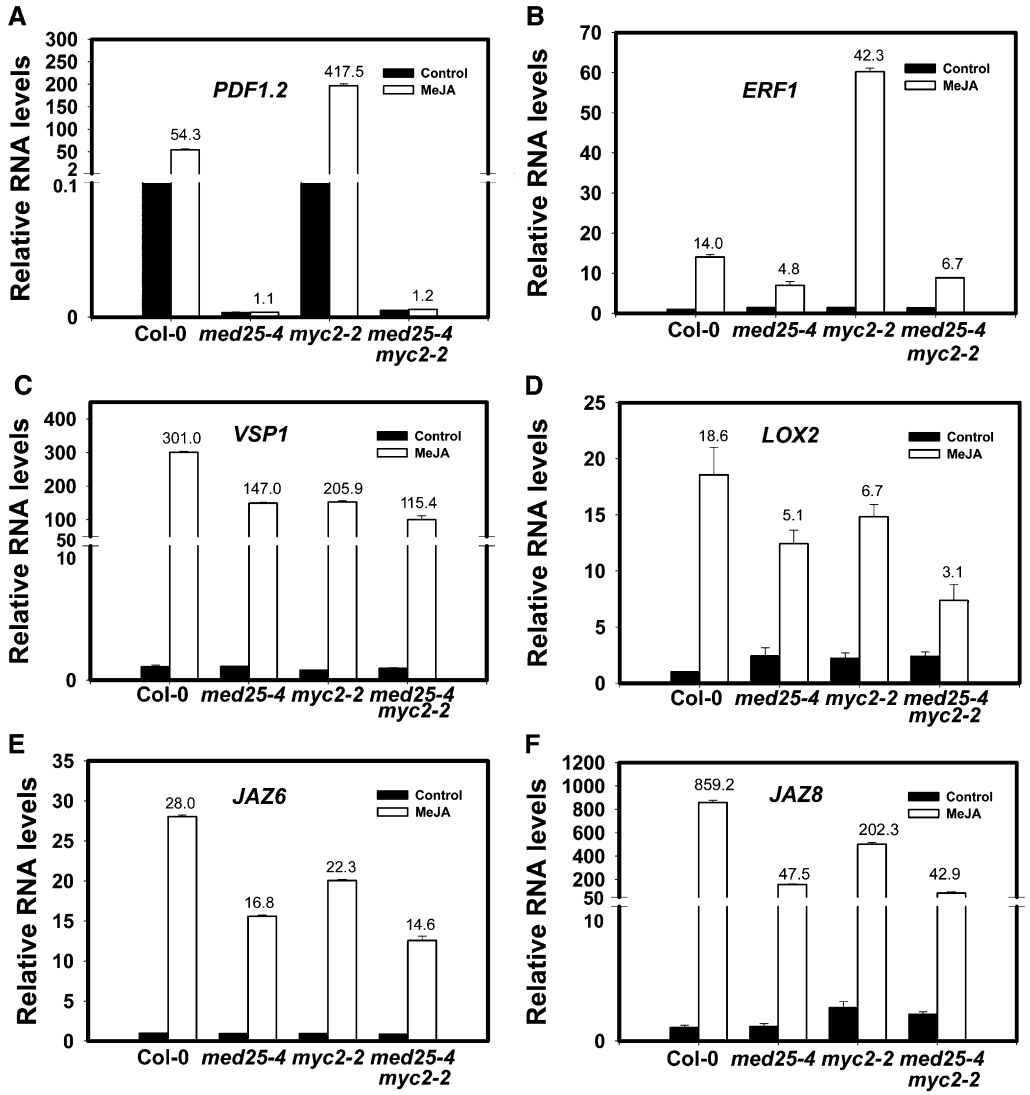

Figure 2. MED25 Affects the Function of MYC2 in Regulating the Transcriptional Expression of JA-Responsive Genes.

Expression of *PDF1.2* (48-h treatments; **[A]**), *ERF1* (1-h treatments; **[B]**), *VSP1* (6-h treatments; **[C]**), *LOX2* (1-h treatments; **[D]**), *JAZ6* (1-h treatments; **[E]**), and *JAZ8* (1-h treatments; **[F]**) was examined by qRT-PCR in Col-0, *med25-4*, *myc2-2*, and *med25-4 myc2-2* plants following 50 μM MeJA treatment. The break ranges (for *PDF1.2*, *VSP1*, and *JAZ8*) are shown on the *y* axis. Data presented are mean values of three biological repeats with SD. Numbers on the white bars represent fold induction values in MeJA-treated plants relative to control (black bars) plants for each genotype.

recruited to the promoter regions of RA-responsive genes and therefore regulates the function of RAR (Lee et al., 2007). In this context, we speculate that the *Arabidopsis* MED25 could associate with MYC2 in chromatin regions of MYC2 target genes. To test this hypothesis, we first assessed the effect of MED25 on the expression JA-responsive genes that are directly targeted by MYC2. It has been shown that in response to JA, MYC2 quickly activates the expression of the *JAZ* family genes via directly binding to the G-box (and T/G-box) sequence in the promoter of these genes (Chini et al., 2007; Hou et al., 2010). Our qRT-PCR assays revealed that the *med25-4* mutation markedly reduced the JA-induced expression levels of the *JAZ* family genes (see Supplemental Figure 2 online). Chromatin immunoprecipitation (ChIP) assays using $35S_{pro}$:*MYC2-GFP* (for green fluorescent protein) plants and anti-GFP antibodies indicated that MYC2 associated with the G-box (5′-CACGTG-3′) motifs in the promoters of *JAZ6* and *JAZ8* (Figures 3A and 3B), confirming that *JAZ6* and *JAZ8* are direct targets of MYC2. ChIP assays using $35S_{pro}$:*MED25-GFP* plants indicated that, like MYC2, MED25 was also enriched in the G-box (5′-CACGTG-3′) motifs of *JAZ6* and *JAZ8* promoters, and, importantly, the enrichment of both MYC2 and MED25 was substantially enhanced by JA treatment (Figure 3B). These results demonstrate that MED25 associates with the transcription factor MYC2 in chromatin regions of MYC2 target genes.

To determine the recruitment dynamic of MYC2 and MED25 to *JAZ* promoters, $35S_{pro}$:*MYC2-GFP* and $35S_{pro}$:*MED25-GFP*

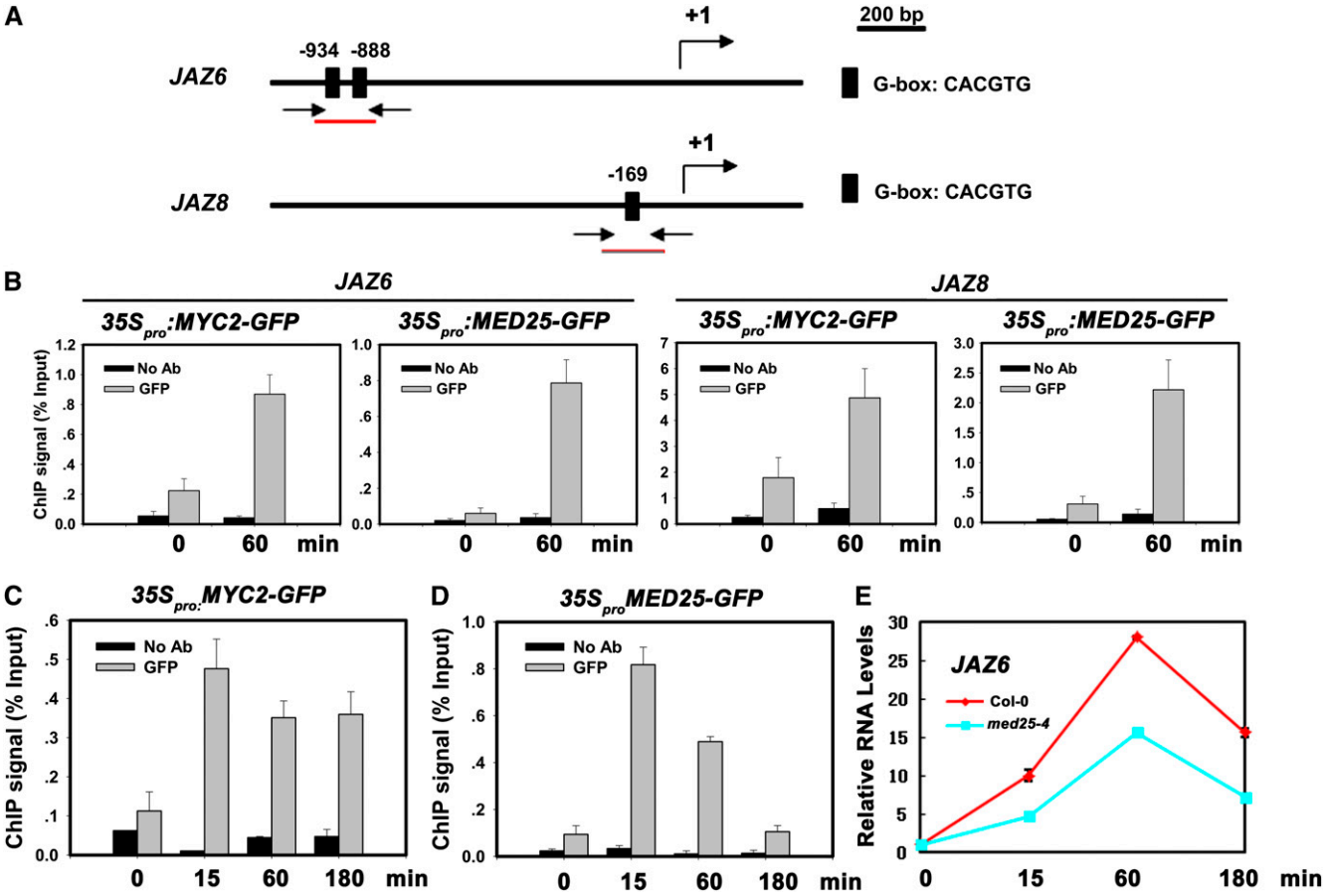

Figure 3. MED25 Is Recruited to Promoter Regions of MYC2 Target Genes in a JA-Dependent Manner.

(A) Schematic diagram of the promoter region of *JAZ6* and *JAZ8*. Black lines represent the promoter region of the two genes. Black boxes on the line represent the putative MYC2 binding G-box (5′-CACGTG-3′); numbers above indicate the distance away from the ATG. Region between the two coupled arrowheads indicates the DNA fragments used for ChIP-PCR. The translational start sites (ATG) were shown as +1. Bar = 200 bp.

(B) Binding of MYC2 and MED25 to *JAZ6* and *JAZ8* promoter regions. The *35S$_{pro}$:MYC2-GFP* and *35S$_{pro}$:MED25-GFP* transgenic seedlings were used in ChIP using anti-GFP antibody (Abcam). For MeJA treatment, *35S$_{pro}$:MYC2-GFP* and *35S$_{pro}$:MED25-GFP* seedlings were treated with 100 μM MeJA for 60 min before cross-linking. The "No Ab" (no antibody) immunoprecipitates served as negative controls. The ChIP signal was quantified as the percentage of total input DNA by real-time PCR. Three biological replicates were performed and identical results were obtained. Standard deviations were calculated from three technical repeats.

(C) and **(D)** Dynamic recruitment of MYC2 and MED25 to *JAZ6* promoter. ChIP assays were performed as in **(B)**, except that *35S$_{pro}$:MYC2-GFP* and *35S$_{pro}$:MED25-GFP* plants were treated with 100 μM MeJA for varying lengths of time (0, 15, 60, and 180 min) before cross-linking.

(E) *JAZ6* mRNA level follows the recruitment pattern of MED25 to the promoter. Col-0 and *med25-4* were treated with MeJA for varying lengths of time (0, 15, 60, and 180 min) as in **(C)** and **(D)**. Data presented are mean values of three biological repeats with SD.

[See online article for color version of this figure.]

plants were incubated with JA for varying lengths of time. ChIP assays indicated that low levels of MYC2 was recruited to *JAZ6* promoter at steady state and that JA treatment leads to a marked increase of MYC2 recruitment within 15 min; MYC2 binding to *JAZ6* promoter then remains at high levels during the time course investigated (Figure 3C). Parallel experiments revealed that MED25 shows negligible association with *JAZ6* promoter at steady state (Figure 3D). In the presence of the ligand, however, MED25 recruitment was quickly increased and reached a maximum within 15 min after JA treatment (Figure 3D); MED25 binding then exhibited a tendency of reduction for the duration of the experiment (Figure 3D). Next, we examined whether the *JAZ6* mRNA levels follow the recruitment pattern of MED25 to the promoter of *JAZ6*. As shown in Figure 3E, in wild-type plants, *JAZ6* mRNA levels increased markedly at 15 min, peaked at 60 min, and then showed a tendency of decrease up to 180 min upon JA treatment. In JA-treated *med25-4* plants, *JAZ6* expression exhibited similar induction kinetics, albeit its expression levels are substantially reduced in *med25-4* compared with those in wild-type plants (Figure 3E). These results indicate that the maximum recruitment of MED25 to the *JAZ6* promoter occurs generally earlier than the peaked activation of *JAZ6* expression. This scenario is consistent with a previous observation in mammalian system showing that Mediator and other coactivators are

targeted to a promoter before significant gene activation occurs (Sharma and Fondell, 2002).

Mapping of the Domains Involved in the MED25/MYC2 Interaction

It has been shown that the MED25 counterparts from animals physically associate with multiple cellular transcriptional activators, including the herpes simplex viral activator VP16 (Mittler et al., 2003; Yang et al., 2004), RAR (Lee et al., 2007), hepatocyte nuclear factor4 (Rana et al., 2011), and the chondrogenesis-related transcriptional activator Sox9 (Nakamura et al., 2011). Our data showing that mutation of the *Arabidopsis MED25* gene affects the action of MYC2 in regulating the expression of JA-responsive genes prompted us to characterize the physical interaction of the two proteins in vivo. Toward this goal, we conducted coimmunoprecipitation (Co-IP) experiments using our recently described *35S$_{pro}$:MYC2-4myc* plants (Chen et al., 2011) and anti-MED25 antibody. Co-IP assays revealed that, in the absence of exogenous JA, MED25 could be precipitated by MYC2 (Figure 4A), suggesting that MED25 interacts with MYC2 at steady state. Parallel Co-IP assays indicated that the precipitation efficiency of MED25 by MYC2 was not substantially changed by JA treatment for 30 min (Figure 4A), suggesting that JA shows little effect on the MED25 and MYC2 interaction at the time point investigated. Next, we tried to map the interaction domain of MED25 with MYC2 using yeast two-hybrid assays. For these experiments, we fused the full length or derivatives of MED25 to the GAL4-DNA binding domain and fused the full-length MYC2 to the GAL4-activation domain (Figure 4B). To circumvent the problem that full-length MED25 can activate the transcription of reporter genes in yeast (Ou et al., 2011), we performed our yeast two-hybrid assays in the presence of 10 mM 3-amino 1,2,4-triazol (Bharti et al., 2000), which could effectively repress the background transcription activation activity of full-length MED25 (see Supplemental Figure 3 online). Under these experimental conditions, we found that full-length MED25 showed interaction with MYC2 in yeast (Figure 4B; see Supplemental Figure 3 online). On the contrary, none of the four individual MED25 domains, including the vWF-A (MED25^{vWF-A}), the MD (MED25^{MD}), the ACID (MED25^{ACID}) and the GD (MED25^{GD}) domains, showed interaction with MYC2 in yeast (Figure 4B). In the context that the ACID domain serves as the ACID of *Arabidopsis* MED25 (Elfving et al., 2011; Ou et al., 2011) as well as its mammalian counterparts (Mittler et al., 2003; Yang et al., 2004; Lee et al., 2007) and that deletion of the ACID and MD, but not of the vWF-A and GD, destroyed MED25 interaction with MYC2 (Figure 4B), we propose that the ACID and the MD are important for MED25 interaction with MYC2. Indeed, the MD-ACID fusion (MED25$^{MD-ACID}$) showed interaction with MYC2 in yeast two-hybrid assays (Figure 4B). We then employed a yellow fluorescent protein (YFP) bimolecular fluorescence complementation (BiFC) system (Weinthal and Tzfira, 2009) to characterize further the MYC2-interacting domain of MED25. Like the full-length MED25 (Figure 4C), the MD-ACID fusion (MED25$^{MD-ACID}$) showed interaction with MYC2 in BiFC assays (Figure 4D). On the contrary, neither MED25^{MD} (Figure 4E) nor MED25^{ACID} (Figure 4F) alone showed interaction with MYC2. Further mapping efforts using BiFC assays revealed that the smallest positive MED25 fragment (MED25$^{540-680}$) included the ACID domain plus 10 amino acids of the MD (Figure 4G). Together, these data indicate that the ACID domain alone is not sufficient for MED25 interaction with MYC2.

We then use yeast two-hybrid assays to map the domain of MYC2 responsible for interaction with MED25. For these experiments, several MYC2 protein derivatives were fused to the GAL4-activation domain and full-length MED25 was fused to the GAL4-DNA binding domain (Figure 4H). As indicated in Figure 4H, the N-terminal part (MYC2$^{1-188}$) containing the putative TAD (MYC2$^{149-188}$) (Lorenzo et al., 2004; Fernández-Calvo et al., 2011) showed interaction with MED25, whereas no interaction was observed using the middle part (MYC2$^{189-445}$) or C-terminal part (MYC2$^{446-624}$). Moreover, the putative TAD of MYC2 alone was sufficient to interact with MED25 (Figure 4H).

It has been shown that in yeast and animals, the Mediator complex physically associates with both DNA-bound transcription factors and Pol II and thus serves as an integrative hub for transcriptional regulation (Malik and Roeder, 2005, 2010; Conaway and Conaway, 2011; Larivière et al., 2012). In this context, our results showing that the *Arabidopsis* MED25 physically associates with MYC2 and strongly affects its function suggests that mutation of *MED25* could impair the recruitment of the general transcriptional machinery during JA-triggered gene transcription. To test this, we assessed the effect of the *med25-4* mutation on JA-induced recruitment of NRPB2 (DNA-directed RNA polymerase II subunit RPB2), the second largest subunit of Pol II (Onodera et al., 2005, 2008; Zheng et al., 2009), to the promoter of MYC2 target genes. Indeed, ChIP assays revealed that JA-induced recruitment of NRPB2 to *JAZ6* promoter was markedly reduced in *med25-4* compared with that in the wild type (Figure 4I).

In a current view of MYC2-directed transcription of JA-responsive genes, it is hypothesized that the JAZ-mediated repression of MYC2 function is achieved through recruitment of the corepressor TPL by NINJA, which physically associates with JAZs (Pauwels et al., 2010). This scenario predicts that during JA response, both MED25 and TPL could be recruited to the promoter of MYC2 targets. Indeed, our ChIP assays revealed that, as with MYC2 (Figures 3B and 3C) and MED25 (Figures 3B and 3D), the TPL corepressor was also recruited to the *JAZ6* promoter (Figure 4J). Importantly, TPL recruitment to *JAZ6* promoter was substantially reduced upon 1 h of JA treatment (Figure 4J), suggesting that TPL recruitment to MYC2 target promoters is regulated by the JA ligand. In addition, Co-IP assays using the reported *35S$_{pro}$:TPL-GFP* plants (Szemenyei et al., 2008) and anti-MED25 antibody indicated that MED25 and TPL could exist in a protein complex (Figure 4K), albeit yeast two-hybrid assays failed to detect their direct physical interaction (see Supplemental Figure 4 online). Taken together, these data support that MED25 may act as part of the general transcriptional machinery in regulating JA-triggered gene expression.

MED25 Negatively Regulates ABA Response during Seed Germination and Early Seedling Growth

Considering that MED25 regulates plant responses to a variety of abiotic stresses (Elfving et al., 2011), in which the phytohormone ABA plays an important regulatory role, we asked whether

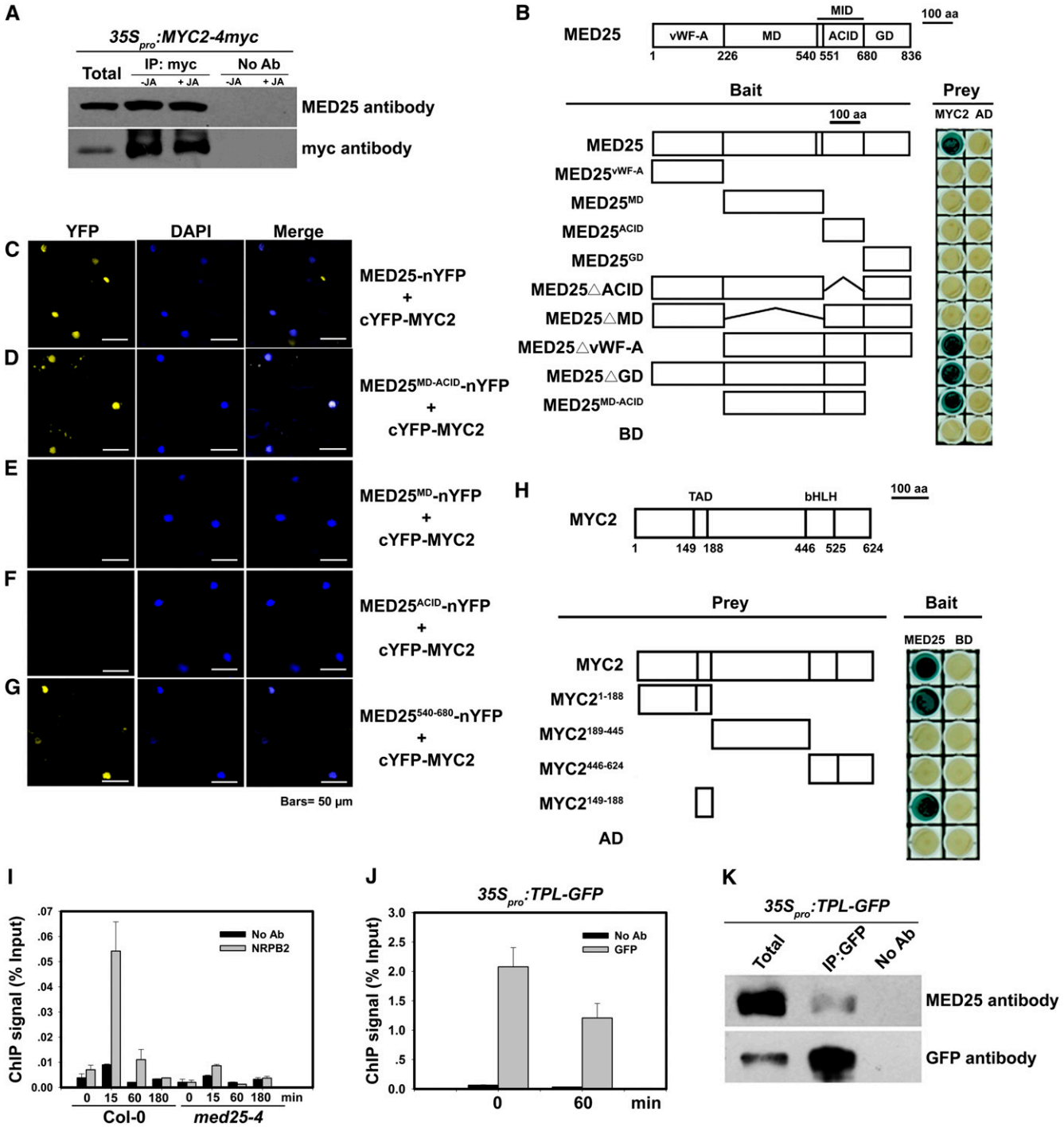

Figure 4. Mapping of Protein Domains Involved in the MED25/MYC2 Interaction.

(A) Co-IP assays showing that MED25 associates with MYC2 in plant cells. Protein extracts from 10-d-old *35S$_{pro}$:MYC2-4myc* seedlings were incubated with (+) or without (−) MeJA (100 μM) for 30 min before immunoprecipitation with myc antibody-bound agarose beads (Santa Cruz). Total and immunoprecipitated proteins were analyzed by immunoblotting using anti-MED25 and anti-myc antibodies. The experiments were repeated three times with similar results.

(B) Mapping of the domains involved in the MED25/MYC2 interaction using yeast two-hybrid assay. Based on the schematic protein structure of MED25 (top panel), full-length MED25 or its derivatives (pGBKT7-MED25 or pGBKT7-MED25 derivatives) were tested for interaction with MYC2 (pGADT7-MYC2) (see Methods for details). Transformed yeast was grown on selective media lacking Ade, His, Leu, and Trp (SD-4) plus X-α-Gal to test protein interactions (left panel). The empty pGADT7 vector was cotransformed with MED25 and its derivatives in parallel as negative controls (right

mutation of *MED25* affects plant response to ABA. In our ABA response assays (Bu et al., 2009; Li et al., 2011), the tested three mutant alleles of *MED25*, including *med25-4*, *pft1-1*, and *pft1-2*, were more sensitive than the wild type to the inhibition effect of ABA in seed germination and early seedling growth (Figures 5A to 5C). Consistent with this, ABA-induced expression levels of *Em1*, *Em6*, and *RAB-RELATED GENE18* (*RAB18*; Lång and Palva, 1992), three ABA-responsive marker genes in *Arabidopsis* (Lopez-Molina et al., 2002), were highly increased in *med25-4* compared with those in the wild type (Figure 5D). These results support that MED25 plays a negative role in regulating ABA responses during seed germination and early seedling growth.

Mutation of *MED25* Affects the Protein Abundance of the ABI5 Transcription Factor

It has been shown that the bZIP transcription factor ABI5 plays a key role in ABA-triggered processes during seed germination and early seedling growth (Lopez-Molina et al., 2001). To examine the genetic interaction between MED25 and ABI5, we generated a double mutant line between *med25-4* and the *abi5-7* mutant, which has been shown to be insensitive to ABA (Figures 5E and 5F) (Bu et al., 2009). Surprisingly, the *med25-4 abi5-7* double mutant exhibits an ABA-insensitive phenotype similar to that of *abi5-7*, indicating that the *abi5-7* mutation suppressed the ABA-hypersensitive phenotype of *med25-4* (Figures 5E and 5F). These genetic data support that the negative effect of MED25 on ABA signaling requires the function of the transcription factor ABI5.

We then examined the possible effect of MED25 on the expression of *ABI5* at both transcription and protein levels. Our qRT-PCR assays revealed that, in germinating seeds (Figure 5G) and 10-d-old seedlings (Figure 5H), the ABA-induced mRNA levels of *ABI5* showed slight but statistically significant decreases in *med25-4* compared with those in the wild type, indicating that MED25 plays a positive role in the ABA-triggered increase of *ABI5* transcripts. These results exclude the possibility that the ABA hypersensitive phenotype of *med25-4* is caused by elevated *ABI5* transcripts. To examine the MED25 effect on *ABI5* expression at the protein level, we crossed the previously described $35S_{pro}$:*ABI5-4myc* (Bu et al., 2009) plants with *med25-4* and generated $35S_{pro}$:*ABI5-4myc*/*med25-4* plants. In line with our previous observations (Bu et al., 2009), $35S_{pro}$:*ABI5-4myc* plants contain a functional *ABI5-4myc* construct (Bu et al., 2009) and therefore exhibit ABA-hypersensitive phenotype (see Supplemental Figure 5 online). It is noteworthy that the ABA hypersensitivity of $35S_{pro}$:*ABI5-4myc*/*med25-4* plants was increased compared with $35S_{pro}$:*ABI5-4myc* plants (see Supplemental Figure 5 online). In our protein gel blot assays, an anti-myc antibody against protein extracts from these seedlings could detect two bands (Figures 5I and 5K), suggesting that the ABI5-4myc fusion protein could exist as different isoforms in these transgenic plants. These results are consistent with previous observations showing that the ABI5 protein mainly accumulates as two isoforms (Lopez-Molina, et al., 2001, 2003; Stone et al., 2006). As shown in Figures 5I and 5J, ABA treatment substantially increased the ABI5-myc fusion protein levels of $35S_{pro}$:*ABI5-4myc* plants. In the *med25-4* background, the ABI5-myc fusion protein levels were already high in the absence of ABA, and no obvious induction was observed in response to ABA treatment (Figures 5I and 5J). These results indicate that MED25 negatively regulates the protein abundance of ABI5. Therefore, the ABA hypersensitivity of *med25-4* coincides with elevated ABI5 protein levels in this mutant. These data, together with our double

Figure 4. (continued).

panel). $MED25^{vWF-A}$, $MED25^{MD}$, $MED25^{ACID}$, and $MED25^{GD}$ represent the vWF-A domain, MD domain, ACID domain, and GD domain of MED25, respectively. MED25△ represents the deletion of certain domains. $MED25^{MD-ACID}$ represents the MD and ACID fusion of MED25. Bar = 100 amino acids (aa).

(C) to **(G)** BiFC assays of MED25 and MYC2 Interaction in *N. benthamiana*. MED25 **(C)**, $MED25^{MD-ACID}$ **(D)**, $MED25^{MD}$ **(E)**, $MED25^{ACID}$ **(F)**, and $MED25^{540-680}$ **(G)** were fused to the N-terminal fragment of YFP (nYFP); MYC2 was fused to the C-terminal fragment of YFP (cYFP). The localization of the nuclei was detected by 4′,6-diamidino-2-phenylindole (DAPI) staining. Bars = 50 μm.

(H) Mapping the MED25-interacting domain of MYC2 in yeast. Based on the schematic protein structure of MYC2 (top panel), MYC2 and its derivatives were fused to the GAL4-activation domain (pGADT7). Full-length MED25 was fused with pGBKT7 as the bait. $MYC2^{149-188}$ represents the putative TAD (transcription activation domain) of MYC2. Bar = 100 amino acids.

(I) ChIP-PCR results showing that the *med25-4* mutation impairs JA-induced recruitment of NRPB2 to the promoter of *JAZ6*. Chromatin was extracted from Col-0 and *med25-4* seedlings after treatment with 100 μM MeJA for varying lengths of time (0, 15, 60, and 180 min) and then was precipitated using anti-RPB2 antibody (Abcam). Precipitated DNA was amplified with primers corresponding to the sequence of the MYC2 binding sites in the promoter of *JAZ6*. The "No Ab" (no antibody) precipitates served as negative controls. The ChIP signal was quantified as the percentage of total input DNA by real-time PCR. Three biological replicates were performed and identical results were obtained. Standard deviations were calculated from three technical repeats.

(J) ChIP-PCR results showing that JA regulates the recruitment of the TPL corepressor to the promoter of *JAZ6*. Chromatin was extracted from $35S_{pro}$:*TPL-GFP* seedlings after treatment with 100 μM MeJA for the indicated length of time and was precipitated using anti-GFP antibody (Abcam). Precipitated DNA was amplified with primers corresponding to the sequence of the MYC2 binding sites in the promoter of *JAZ6*. The "No Ab" (no antibody) precipitates served as negative controls. ChIP data analysis was the same as in **(I)**.

(K) Co-IP results showing that TPL and MED25 could exist in a protein complex. Protein extracts from 6-d-old $35S_{pro}$:*TPL-GFP* seedlings were immunoprecipitated (IP) with or without GFP antibody, followed by addition of protein G plus agarose beads to capture the protein complex. Total and immunoprecipitated proteins were analyzed by immunoblotting using anti-MED25 and anti-GFP antibodies. The experiments were repeated three times with similar results.

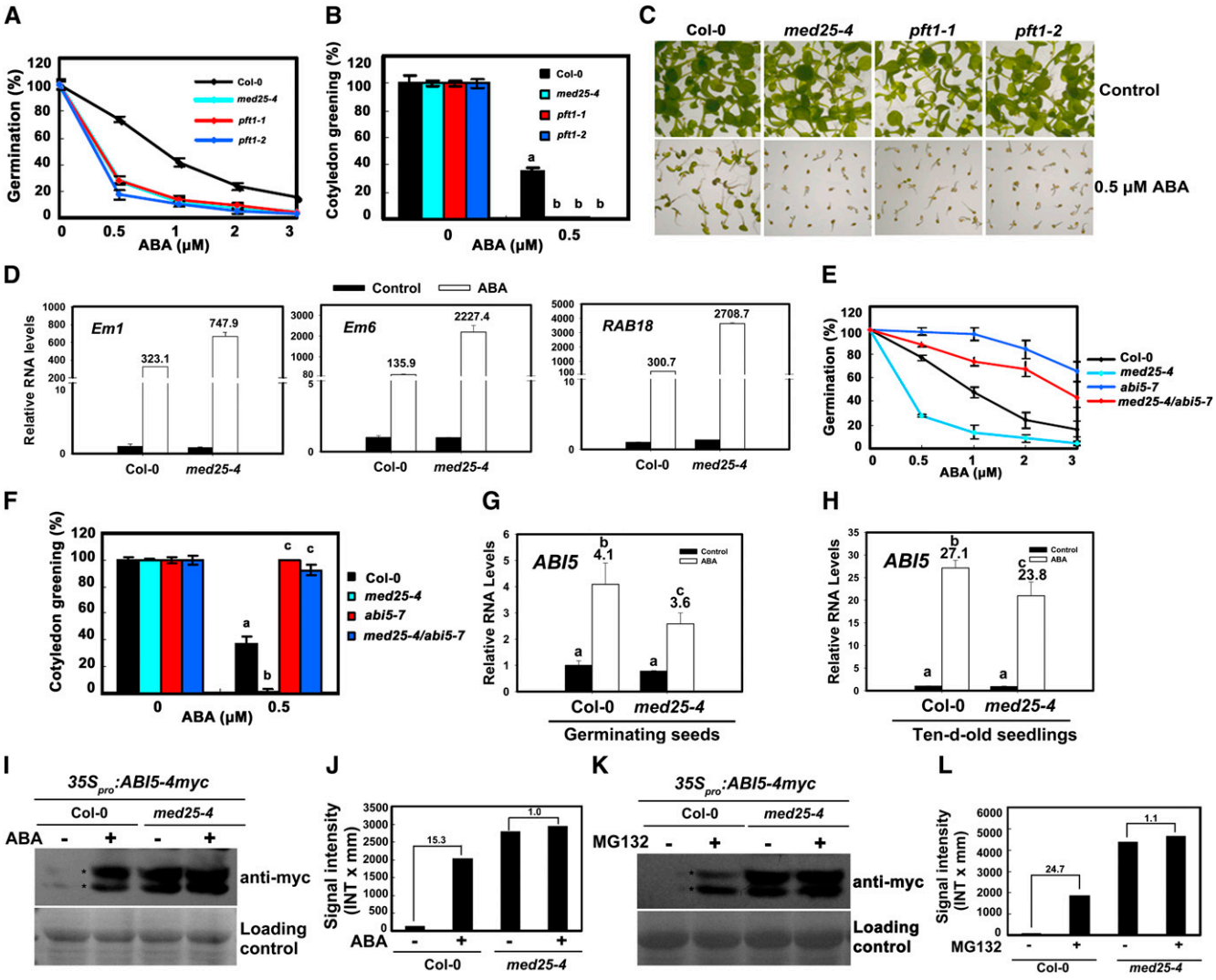

Figure 5. MED25 Negatively Regulates ABA Responses during Seed Germination and Early Seedling Growth.

(A) Quantification of seed germination. Seed germination percentage of the indicated genotypes grown on different concentrations of ABA was recorded at 3 d after the end of stratification. Data shown are mean ± SD of three replicates. At least 100 seeds per genotype were measured in each replicate.

(B) Quantification of cotyledon greening. Cotyledon-greening percentage of the indicated genotypes grown on medium containing 0.5 μM ABA was recorded at 5 d after the end of stratification. Data shown are mean ± SD of three replicates. At least 100 seeds per genotype were measured in each replicate. Cotyledon greening variance on ABA medium was analyzed by Fisher's LSD mean separation test (SPSS). Samples with the different letters are significantly different at $P < 0.01$.

(C) Photographs showing the ABA hypersensitivity of *med25* alleles in early seedling growth. Growth conditions are the same as **(B)**, and photos were taken 7 d after stratification. Cotyledons of Col-0 all turned green at that stage.

(D) qRT-PCR analyses of ABA-responsive genes. Seeds were kept in darkness at 4°C for 3 d without ABA and then transferred to 10 μM ABA plates for 3 d. Germinating seeds were collected for RNA extraction using the RNAqueous kit (Ambion) for small-scale RNA isolation. Data shown are mean values of three biological repeats with SD. Control indicates the time immediately following transfer. Numbers on the white bars represent fold induction values in ABA-treated plants relative to control (black bars) plants.

(E) Quantification of seed germination in the *med25-4 abi5-7* double mutant. Seed germination percentage of the indicated genotypes grown on different concentrations of ABA was recorded at 3 d after the end of stratification. Data shown are mean ± SD of three replicates. At least 100 seeds per genotype were measured in each replicate.

(F) Quantification of cotyledon greening in the *med25-4 abi5-7* double mutant. Cotyledon greening percentage of the indicated genotypes grown on medium containing 0.5 μM ABA was recorded at 5 d after the end of stratification. Data shown are mean ± SD of three replicates. At least 100 seeds per genotype were measured in each replicate. Cotyledon greening variance on ABA medium was analyzed by Fisher's LSD mean separation test (SPSS). Samples with the different letters are significantly different at $P < 0.01$.

mutant analysis between *med25-4* and the *abi5-7*, support a hypothesis that the ABA hypersensitive phenotype of *med25-4* is caused by the elevated ABI5 protein abundance.

We then asked whether 26S proteasome-dependent proteolysis is involved in the above-described MED25-mediated modulation of ABI5-myc protein abundance. Consistent with a previous report that the ABI5 protein is subject to 26S proteasome–mediated protein degradation (Lopez-Molina et al., 2001), we found that MG132 treatment led to an obvious increase of the ABI5-myc fusion protein in $35S_{pro}$:*ABI5-4myc* plants (Figures 5K and 5L). In $35S_{pro}$:*ABI5-4myc*/*med25-4* plants, the ABI5-myc fusion protein levels were already high and only a mild increase was observed upon MG132 treatment (Figures 5K and 5L). These results support the fact that MED25-mediated increase of ABI5 protein abundance possibly involves the 26S proteasome-mediated proteolysis system.

ABA Affects the Recruitment of ABI5 and MED25 to Promoters of ABI5 Targets

We then used ChIP assays to examine whether MED25 is recruited to promoters of ABI5 target genes during ABA signaling. As shown in Figure 6A, the promoter region of *Em6* contains a G-box type abscisic acid–responsive element (ABRE), which has been shown to be targeted by ABI5 (Carles et al., 2002). Time-course ChIP assays using $35S_{pro}$:*ABI5-4myc* plants revealed that, in the absence of ABA, a low amount of ABI5 bound to the chromatin region covering the G-box type ABRE of the *Em6* promoter (Figure 6B). Binding of ABI5 to *Em6* promoter was clearly enhanced 1 h after ABA treatment, and this ABA-induced enhancement showed a tendency to increase during the time course investigated (Figure 6B). In a parallel time-course ChIP experiment, we use the $35S_{pro}$:*MED25-4myc* plants to investigate the ABA dependency of MED25 recruitment to the same region of *Em6* promoter. Significantly, we found that, in contrast with ABI5, MED25 was highly enriched in the *Em6* promoter in the absence of ABA; in response to ABA treatment, MED25 recruitment to the *Em6* promoter exhibited a trend of decrease for the duration of the experiment (Figure 6C).

Mapping of the Domains Involved in the MED25/ABI5 Interaction

BiFC assays revealed that full-length MED25 interacts with full-length ABI5 in *Nicotiana benthamiana* leaves (Figure 6D). Physical interaction between MED25 and ABI5 was confirmed by Co-IP experiments using $35S_{pro}$:*ABI5-4myc* plants and anti-MED25 antibody. As shown in Figure 6E, MED25 could be precipitated by ABI5 in the absence of exogenous ABA, suggesting that MED25 interacts with ABI5 at steady state. Significantly, Co-IP assays also revealed that, 3 h after ABA treatment, the precipitation efficiency of MED25 by ABI5 was substantially reduced, suggesting that ABA attenuates the interaction between ABI5 and MED25. These results are consistent with the above-described time-course ChIP data showing that the MED25 enrichment to the ABI5 targets was reduced by ABA (Figure 6C). We then examined the domains involved in MED25 and ABI5 interaction using yeast two-hybrid assays. As shown in Figure 6F, MED25 interacts with ABI5 in yeast, and the ACID domain of MED25 is sufficient for this interaction. It is noteworthy that even though the ACID domain itself is not sufficient for MED25 interaction with MYC2, this domain is sufficient for MED25 interaction with ABI5, suggesting that the action mechanisms of MED25 in regulating JA and ABA signaling are different. To map the MED25-interacting domain of ABI5, we generated several ABI5 derivatives based on previous functional analyses of the ABI5 protein (Bensmihen et al., 2002; Lopez-Molina et al., 2003). Interestingly, we found that the ABI5 C-terminal part, but not its N-terminal part containing the TAD ($ABI5^{9\text{-}122aa}$) (Nakamura et al., 2001), showed interaction with MED25 (Figure 6G). We further delimited the MED25 interaction domain of ABI5 to amino acids 221 to 349 ($ABI5^{221\text{-}349}$) (Figure 6G).

DISCUSSION

Upon perception by plant cells, phytohormones trigger genome-wide transcriptional reprogramming. Regulated gene expression therefore plays a central role in hormone signaling. While much effort in the field of hormone signaling is devoted to gene-specific transcription factors, we know relatively little about the function of

Figure 5. (continued).

(G) qRT-PCR analyses of *ABI5* expression in germinating seeds. Assays were performed as in **(D)**. Data shown are mean values of three biological repeats with SD. Control indicates the time immediately following transfer. Numbers on the white bars represent fold induction values in ABA-treated plants relative to control (black bars) plants.

(H) qRT-PCR analyses of *ABI5* expression in 10-d-old seedlings. Col-0 and *med25-4* were treated with or without 100 μM ABA for 6 h. Data shown are mean values of three biological repeats with SD. Numbers on the white bars represent fold induction values in ABA-treated plants relative to control (black bars) plants.

(I) and **(J)** Immunoblot and quantitative analyses of the ABI5-myc protein. Ten-day-old $35S_{pro}$:*ABI5-4myc*/Col-0 and $35S_{pro}$:*ABI5-4myc*/*med25-4* seedlings were treated with (+) or without (−) 100 μM ABA in liquid half-strength MS for 6 h. Proteins were extracted and the indicated protein levels were determined by immunoblot assays using myc antibody (Abmart). Asterisks indicate the two predominant bands of ABI5-myc protein. The levels of ABI5-myc proteins in **(I)** were quantified by Quantity One (Bio-Rad) software. The band quantity was measured by the area under its Gaussian-fitted profile. Units are intensity (INT) × mm. The signal intensity of each band was calculated and added together as the whole signal intensity of ABI5-myc proteins **(J)**. These experiments were repeated three times with similar results.

(K) and **(L)** Immunoblot and quantitative analyses of the ABI5-myc protein. Ten-day-old $35S_{pro}$:*ABI5-4myc*/Col-0 and $35S_{pro}$:*ABI5-4myc*/*med25-4* seedlings were treated with (+) or without (−) 100 μM MG132 in liquid half-strength MS for 24 h. The levels of ABI5-myc proteins **(K)** were quantified in **(L)**. These experiments were repeated three times with similar results.

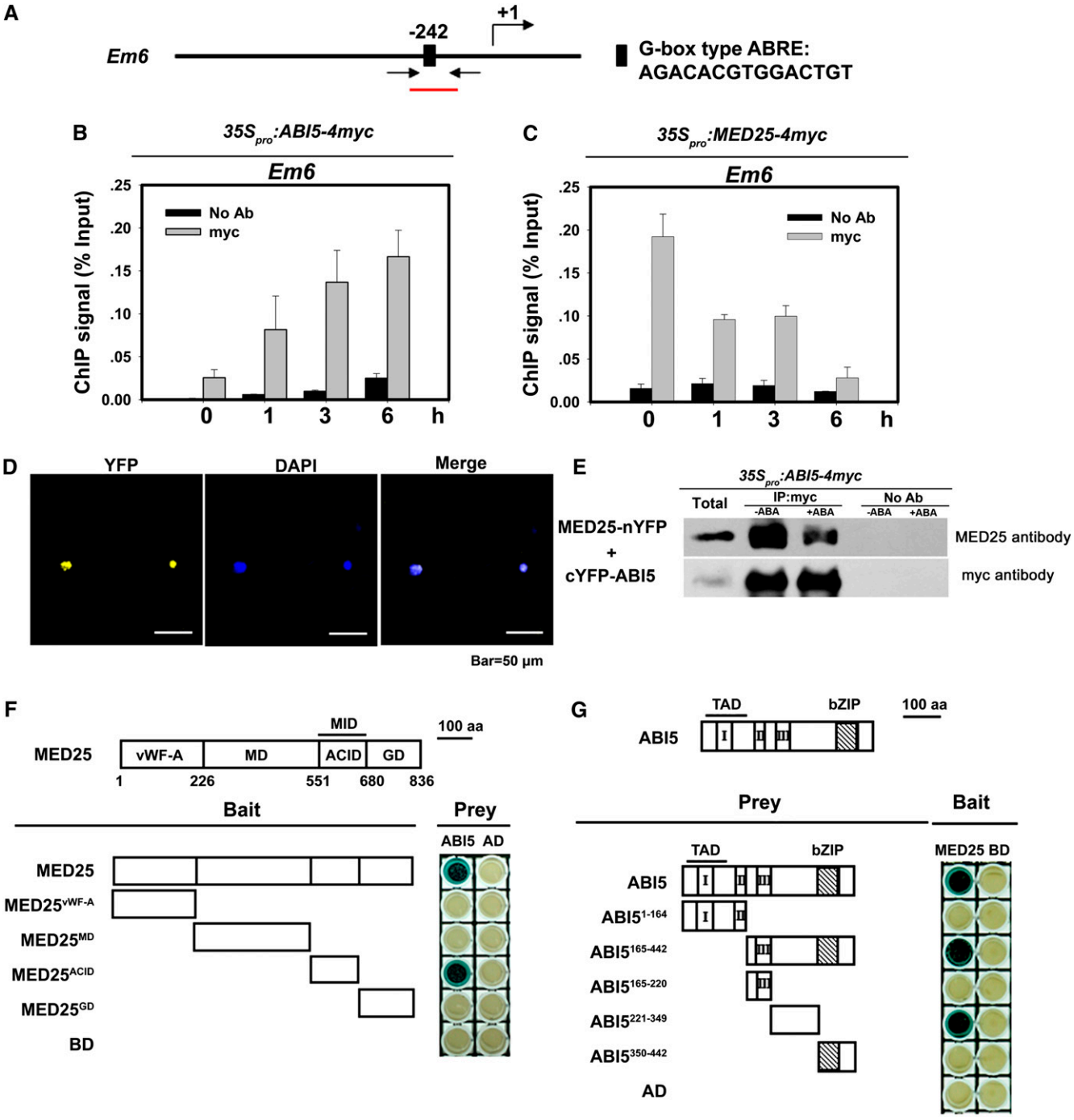

Figure 6. MED25 Associates with ABI5 in Promoter of ABI5 Target Genes.

(A) Schematic diagram of the promoter region of *Em6*. Black line represents the promoter region of the gene. Black box on the line indicates the putative ABI5 binding G-box type ABRE *cis*-element of *Em6* promoter (Carles et al., 2002). Region between the two coupled arrowheads (red line) indicates the DNA fragments used for ChIP-PCR. The translational start sites (ATG) are shown as +1. Bar = 200 bp.

(B) and **(C)** Time-course ChIP assays showing the dynamic recruitment of ABI5 **(B)** and MED25 **(C)** to *Em6* promoter. The $35S_{pro}$:*ABI5-4myc* and $35S_{pro}$:*MED25-4myc* transgenic seedlings were used in ChIP using anti-myc antibody (Millipore). $35S_{pro}$:*ABI5-4myc* or $35S_{pro}$:*MED25-4myc* seedlings were treated with 100 μM ABA for varying lengths of time (0, 1, 3, and 6 h) before cross-linking. The "No Ab" (no antibody) immunoprecipitates served as negative controls. The ChIP signal was quantified as the percentage of total input DNA by real-time PCR. Three biological replicates were performed and identical results were obtained. Standard deviations were calculated from three technical repeats.

protein complexes that interact with the RNA polymerase during gene transcription, such as the Mediator complex. The Mediator complex has only recently been isolated from plant cells, and diverse functions, including development (Autran et al., 2002; Wang and Chen, 2004; Gillmor et al., 2010; Ito et al., 2011; Xu and Li, 2011), stress responses (Cerdán and Chory, 2003; Kidd et al., 2009; Elfving et al., 2011), and noncoding RNA production (Kim et al., 2011), have been attributed to plant Mediator subunits. In this study, we provide evidence showing that MED25, a multifunctional subunit of the *Arabidopsis* Mediator complex, differentially regulates JA and ABA signaling through distinct interaction mechanisms with hormone-specific transcription factors.

MED25 Plays a Positive Role in MYC2-Regulated Expression of JA-Responsive Genes

MED25 was originally identified as PHYTOCHROME AND FLOWERING TIME1 (PFT1), which plays an important role in the regulation of flowering time in response to light quality (Cerdán and Chory, 2003). Biochemical purification of the *Arabidopsis* Mediator revealed that PFT1 is homologous to the MED25 subunit of the metazoan Mediator complex (Bäckström et al., 2007). Later it was reported that MED25 is also involved in plant defense responses to a variety of biotic (Kidd et al., 2009) and abiotic (Elfving et al., 2011) stresses. More recently, MED25 was shown to be important for the control of final organ size (Xu and Li, 2011). These studies suggest that, like its animal counterparts (reviewed in Borggrefe and Yue, 2011), the *Arabidopsis* MED25 subunit plays multiple roles in plant development, hormone signaling, and stress responses. Notably, however, the molecular mechanisms underlying the diverse functions of MED25 remain largely unknown.

Our investigation of the MED25 function in JA signaling is focused on its interplay with MYC2, a master transcription factor regulating diverse aspects of JA-responsive gene expression. In line with a recent report that MED25 is important for JA-induced defense responses to pathogen infection (Kidd et al., 2009), we provide several lines of evidence showing that MED25 facilitates the action of MYC2 in regulating JA-induced defense gene expression. First, MED25 positively influences the function of MYC2 in regulating the expression of both wound- and pathogen-responsive genes. Second, double mutant analyses reveal that MED25 acts genetically downstream from MYC2 in regulating the expression of JA-responsive genes. Third, MED25 physically interacts with the putative TAD of MYC2. Fourth, MED25 and MYC2 are recruited to promoter regions of MYC2 target genes at roughly the same time after JA treatment. The above-described action mode of *Arabidopsis* MED25 in regulating MYC2-mediated transcription shows high similarity to that of its human counterpart in regulating RAR-mediated transcription. It has been well established that in the presence of RA, the RAR ligand, human MED25 is recruited to promoter regions of RAR targets and, through direct interaction with RAR, imposes a positive effect on RAR transcriptional activation (Lee et al., 2007). Together, these data support that MED25 might act as a coactivator of MYC2 in regulating JA-induced defense gene expression. Significantly, we provide evidence showing that, in response to JA, a Pol II subunit is recruited to the promoter of MYC targets in a MED25-dependent manner. In addition, we show that, the TPL corepressor, which is involved in JAZ-mediated repression of MYC2 function (Pauwels et al., 2010), is associated with MED25 in the promoter of MYC2 targets. These results together support that MED25 acts as part of the general transcriptional machinery in regulating JA-triggered gene expression. It will be interesting in future studies to elucidate the molecular details of how MED25 coordinates the actions of numerous coactivators and corepressors and therefore facilitates MYC2-dependent regulation of JA-responsive genes. It was shown that the transcription factor ETHYLENE INSENSITIVE3 (EIN3) and its closest homolog EIN3-LIKE1 (EIL1) integrate ethylene and JA signaling in defense gene expression (Zhu et al., 2011). This study demonstrates that, in the absence of JA, EIN3/EIL1 are repressed by JAZs, which recruit HDA6 (for histone deacetylase6) as a corepressor. JA enhances the transcriptional activity of EIN3/EIL1 by removal of JAZ proteins to regulate gene expression (Zhu et al., 2011). It is of significance to examine the possible association of MED25 with EIN3/EIL1, JAZs, and HDA6 in the promoter of EIN3/EIL1 target genes.

Notably, a recent study found that MED25 also interacts with several other JA-responsive transcription factors, including ETHYLENE RESPONSE FACTOR1 (ERF1) (Ou et al., 2011), suggesting that MED25 integrates multiple signals from different JA-responsive transcription factors during JA-induced gene expression. In the context that *ERF1* itself is a direct target of MYC2 and that the negative regulation of *PDF1.2* by MYC2 is

Figure 6. (continued).

(D) BiFC assay of MED25 and ABI5 interaction in *N. benthamiana*. MED25 was fused to the N-terminal fragment of YFP (nYFP), and ABI5 was fused to the C-terminal fragment of YFP (cYFP). DAPI, 4′,6-diamidino-2-phenylindole. Bar = 50 μm.

(E) Co-IP results showing that ABA attenuates the interaction of MED25 with ABI5. Protein extracts from 10-d-old $35S_{pro}$:*ABI5-4myc* seedlings were incubated with or without (±) ABA for 3 h before immunoprecipitation using myc antibody-bound agarose beads (Santa Cruz Biotechnology). Total and immunoprecipitated proteins were analyzed by immunoblotting using anti-MED25 and anti-myc antibodies. The experiments were repeated three times with similar results.

(F) The ACID domain of MED25 interacts with ABI5. Based on the schematic protein structure of MED25, full-length MED25 or its derivatives (pGBKT7-MED25 or pGBKT7-MED25 derivatives) were tested for interaction with ABI5 (pGADT7-ABI5). Bar = 100 amino acids (aa).

(G) Mapping the MED25-interacting domain of ABI5 in yeast. The conserved domains of ABI5 are depicted as I, II, and III (Bensmihen et al., 2002; Lopez-Molina et al., 2003); box with bias in the C-terminal region indicates the bZIP domain. ABI5 and its derivatives were fused to the GAL4-activation domain (pGADT7). Full-length MED25 was fused with pGBKT7 as the bait. Bar = 100 amino acids.

mediated by suppression of *ERF1*, which in turn directly binds to the *PDF1.2* promoter (Dombrecht et al., 2007; Zarei et al., 2011), it is reasonable to speculate that, upon JA induction, MED25 is recruited in a sequential manner to targets of MYC2 and to targets of a spectrum of intermediate JA-responsive transcription factors. In line with this hypothesis, our time-course ChIP assays indicated that MED25 accumulation in MYC2 direct targets showed an obvious reduction at 60 min after JA treatment. We are currently aiming to understand the molecular mechanisms underlying the dynamic recruitment of MED25 to targets of different JA-responsive transcription factors.

MED25 Plays a Negative Role in ABI5-Regulated Expression of ABA-Responsive Genes

Our investigation of the MED25 function in ABA signaling is focused on its genetic and physical interaction with the bZIP transcription factor ABI5, an important regulator of the ABA signaling during seed germination and early seedling growth. Surprisingly, we found that the MED25 effect on ABA signaling distinguishes its effect on JA signaling in several aspects. First, in contrast with a positive effect on MYC2-dependent JA responses, MED25 negatively regulates ABI5-dependent ABA responses. Second, our double mutant analyses reveal that, whereas MED25 acts genetically downstream of MYC2 in JA signaling, this Mediator subunit acts genetically upstream of ABI5 during ABA-mediated seed germination and early seedling development. Third, whereas the putative TAD of MYC2 is involved in MED25/MYC2 interaction, the TAD of ABI5 is not involved in MED25/ABI5 interaction. Fourth, time-course ChIP assays indicate that the basal recruitment of MED25 to MYC2 target promoters is relatively low, and JA treatment substantially stimulates the binding of MED25 to chromatins of MYC2 targets. By contrast, MED25 was highly enriched in ABI5 target promoters at steady state and ABA treatment led to reduction of this enrichment. These results together suggest that, as a coregulator of transcription factors, MED25 employs distinct mechanisms to affect the function of ABI5 and MYC2.

Considering that MED25 imposes an overall negative effect on ABI5-dependent ABA responses, our investigation of the recruitment dynamics of ABI5 and MED25 to the *Em6* promoter provides clues to understand how the ABI5–MED25 interaction coordinates ABI5-directed gene expression. In the absence of ABA, ABI5 accumulation at its target promoter is low, whereas MED25 accumulation at the same promoter region is high, which keeps ABI5-regulated gene expression at low levels. ABA treatment stimulates the recruitment of ABI5 to its target promoter and, at the same time, leads to reduced recruitment of MED25 to the same promoter region. Increased ABI5 and reduced MED25 both favor ABI5-regulated gene expression at high levels.

Intriguingly, our study reveals that the mode of action of MED25 on ABI5 is complex. On one hand, MED25 positively regulates ABA-induced *ABI5* expression at the transcription level. On the other hand, MED25 negatively regulates ABI5 expression at the protein level. In addition, we could not exclude the possibility that MED25 interacts with ABI5 and, therefore, negatively affects ABI5-dependent induction of its target genes. This latter effect could be achieved through MED25-dependent recruitment of transcription cofactors to the promoter region of ABI5 targets. It has been shown that during RA signaling in human cells, CREB binding protein/p300, a histone acetyltransferase, was recruited in a MED25-dependent manner to the promoter region of RAR targets and therefore cooperates in RAR activation (Lee et al., 2007).

An interesting aspect of the MED25 function in ABA responses concerns its effect on the protein accumulation and stability of ABI5, which has been considered as a checkpoint of ABA-mediated arrest of seed germination and early seedling growth (Lopez-Molina et al., 2001; Fujita et al., 2011). In the context that the *Arabidopsis* Mediator complex contains a detachable kinase module, which is composed of the cyclin-dependent kinase Cdk8, Cyclin C, and two additional subunits, MED12 and MED13 (Bäckström et al., 2007; Kidd et al., 2011; Kim and Chen, 2011), it is reasonable to speculate that MED25, or other relevant Mediator subunits, regulate the phosphorylation and/or protein degradation of ABI5. It will be interesting in future studies to elucidate the molecular mechanisms concerning MED25-mediated regulation of ABI5 protein modification and/or degradation.

MED25 Is an Interaction Node between JA and ABA Signaling Pathways

JA and ABA are phytohormones involved in plant responses to biotic and abiotic stresses, and it is increasingly evident that significant interactions occur between these pathways. Our finding that MED25 positively regulates JA signaling whereas it negatively regulates ABA signaling highlights the existence of an antagonistic interaction between JA and ABA in regulating seed germination. In line with this, early studies indicate that several of the JA-insensitive mutants, including *jar1*, *ja insensitive4*, and *coi1-16*, show increased sensitivity to low concentrations of ABA in seed germination, suggesting that JA antagonizes ABA in regulating the onset of seed germination (Staswick et al., 1992; Berger et al., 1996; Ellis and Turner, 2002). This long-observed antagonistic interaction between JA and ABA could be employed to identify molecular components of ABA signaling in seeds. For example, several ABA-related mutants named *coi1-16 resistant to ABA* have been recovered based on their ability to suppress the hypersensitive phenotype of *coi1-16* to low concentrations of ABA in seed germination (Fernández-Arbaizar et al., 2012). Characterization of these mutants promises to shed new light on the molecular mechanism governing JA and ABA interactions in regulating seed germination and early seedling growth.

Intriguingly, however, JA has also been shown to have a synergistic effect with ABA in regulating seed germination. For example, both hormones induce the expression of *MYC2*, which plays a positive role in both JA- and ABA-mediated inhibition of seed germination (Abe et al., 2003; Lorenzo et al., 2004). Considering that the induction of *MYC2* by ABA depends on the JA receptor COI1, it is likely that ABA activates the expression of MYC2 by the JA signaling pathway (Lorenzo et al., 2004).

Previous studies have also observed both antagonistic and cooperative interactions between JA and ABA in regulating plant

resistance to different pathogens. For example, it was shown that ABA antagonizes JA-induced expression of defense-related genes and that *Arabidopsis* mutants defective in ABA biosynthesis or signaling show increased resistance to the fungal pathogen *Fusarium oxysporum* (Anderson et al., 2004), suggesting a negative role of ABA in plant resistance to *F. oxysporum*. By contrast, it was shown that ABA activates JA biosynthesis and therefore plays a positive role in resistance of *Arabidopsis* plants to the oomycete pathogen *Pythium irregulare* (Adie et al., 2007). The differential role of ABA within different plant–pathogen interactions implies that this hormone could be important for the fine-tuning of plant resistance to a particular pathogen.

METHODS

Plant Materials and Growth Conditions

Arabidopsis thaliana ecotype Col-0 was used as the wild type. Some of the plant materials used in this study were previously described: *ber6/med25-4* (Zheng et al., 2006); *med25-1*, *med25-2*, and *med25-3* (Xu and Li, 2011); *pft1-1* (Cerdán and Chory, 2003); *pft1-2* (Kidd et al., 2009); *myc2-2* (Boter et al., 2004); *coi1-2* (Xu et al., 2002); *abi5-7* (Nambara et al., 2002; Tamura et al., 2006); $VSP1_{pro}$:*GUS* and $PDF1.2_{pro}$:*LUC* (Zheng et al., 2006); $35S_{pro}$:*MYC2-4myc* (Chen et al., 2011); $35S_{pro}$:*ABI5-4myc* (Bu et al., 2009); and $35S_{pro}$:*TPL-GFP* (Szemenyei et al., 2008).

The *med25-4 myc2-2* and *med25-4 abi5-7* double mutants were generated by crossing parental single homozygous lines. The resulting F2 segregating progenies were genotyped to identify plants homozygous for each locus. The *med25-4* and *myc2-2* (Salk_083483) mutations were identified with PCR-based markers (see Supplemental Figure 1 online). Identification of the *abi5-7* mutation was previously described (Bu et al., 2009).

Arabidopsis plants were grown in Murashige and Skoog (MS) medium at 22°C with a 16-h-light/8-h-dark photoperiod (light intensity 120 μM photons m^{-2} s^{-1}) as previously described (Sun et al., 2009). JA-mediated root growth inhibition assays were described (Chen et al., 2011). For ABA responses, seeds harvested at the same time were used for the germination and cotyledon greening assays as recently described (Bu et al., 2009; Li et al., 2011). *Nicotiana benthamiana* was grown under a 16-h-light (28°C)/8-h-dark (22°C) photoperiod.

Map-Based Cloning of *BER6*

The *ber6/med25-4* (Col-0) mutant was crossed to Landsberg *erecta*. In the resulting F2 population, individuals showing the *ber6* phenotype (i.e., insensitivity to JA-induced root growth inhibition) were identified and used for mapping. Rough mapping using 30 plants indicated that the target gene is linked to the marker ciw12 on chromosome 1. New markers (see Supplemental Table 1 online) in this region were designed according to the Monsanto *Arabidopsis* polymorphism database (http://www.Arabidopsis.org/browse/Cereon/). Using these markers, we analyzed 1800 plants showing the mutant phenotype and delimited the target gene to a 50-kb region covered by the BAC clone F2J7 (Figure 1H). Among the 15 genes in this region, sequencing analyses revealed a G-to-A mutation in the *MED25* gene (At1g25540).

For complementation analysis, the $35S_{pro}$:*MED25-GFP* construct was introduced into the *ber6* plants using *Agrobacterium tumefaciens*–mediated transformation.

For the allelic test, the *ber6/med25-4* mutant was crossed to the previously characterized *pft1-2* mutant (Kidd et al., 2009), and the resulting F1 plants were examined.

Measurement of Flowering Time

Measurements of flowering time were performed as previously described (Robson et al., 2010). Flowering time was recorded from at least 20 plants per genotype that were grown in soil under either long days (16 h white light/8 h dark) or short days (10 h white light/14 h dark). Flowering time was scored as the number of days from germination to the first appearance of buds at the apex. The total number of rosette leaves was counted after the main stem has bolted 1 cm.

DNA Constructs and Plant Transformation

DNA constructs for plant transformation were generated following standard molecular biology protocols and Gateway (Invitrogen) technology. Full-length coding sequence of *MED25* was amplified with Gateway-compatible primers. The PCR product was cloned by pENTR Directional TOPO cloning kits (Invitrogen) and then recombined with the binary vector pGWB5 (35S promoter, *C-GFP*) to generate the $35S_{pro}$:*MED25-GFP* construct. Full-length coding sequence of *MED25* was also cloned into the pGWB17 vector (35S promoter, C-4myc) to generate the $35S_{pro}$:*MED25-4myc* construct. Similarly, we generated the $35S_{pro}$:*MYC2-GFP* construct. All primers used for DNA construct generation are listed in Supplemental Table 2 online.

The above constructs were then transformed into *Agrobacterium* strain GV3101 (pMP90), which was used for transformation of *Arabidopsis* plants via a floral dip method. Transformants were selected based on their resistance to hygromycin. Homozygous T3 or T4 transgenic seedlings were used for phenotype and molecular characterization.

Yeast Two-Hybrid Assays

Full-length coding sequence of MED25 and its derivatives were amplified with listed primers (see Supplemental Table 2 online). Enzyme-digested PCR products were cloned into the same site of pGBKT7. Full- length MYC2, ABI5, and their derivatives were also amplified with listed primers (see Supplemental Table 2 online) and cloned into pGADT7. Yeast two-hybrid assays were based on Matchmaker GAL4 two-hybrid systems (Clontech). Constructs to test interaction were cotransformed into the yeast strain *Saccharomyces cerevisiae* AH109. The presence of the transgenes was confirmed by growth on an SD/-Leu/-Trp plate. To assess protein interactions, the transformed yeasts were suspended in liquid SD/-Leu/-Trp to OD = 1.0. Five microliters of suspended yeast was spread in a well on the 96-well plates containing SD/-Ade/-His/-Leu/-Trp/ X-α-Gal (4 mg/mL) medium. The interactions were observed after 3 d of incubation at 30°C. To circumvent the problem that full-length MED25 can activate the transcription of reporter genes in yeast, we performed our yeast two-hybrid assays in the presence of 10 mM 3-amino 1,2,4-triazol (Bharti et al., 2000), which can effectively repress the background transcription activation activity of full-length MED25 (see Supplemental Figure 3 online). The experiments were repeated three times with similar results.

To test the possible interaction of MED25 with TPL and NINJA, the full-length coding sequences of MED25, NINJA, and JAZ1 were cloned into pGADT7, and the full-length coding sequences of TPL and NINJA were cloned into pGBKT7. Primers used are listed in Supplemental Table 2 online.

Co-IP Assays

Co-IP assays were performed according to published procedure (Spoel et al., 2009) with minor modifications. In brief, 10-d-old $35S_{pro}$:*MYC2-4myc* seedlings were homogenized in protein lysis buffer (50 mM Tris-HCl, pH 7.5, 150 mM NaCl, 0.1% Triton X-100, 0.2% Nonidet P-40, 0.6 mM PMSF, and 20 μM MG132 with Roche protease inhibitor cocktail). After protein extraction, 20 μL protein G plus agarose (Santa Cruz) was added

to the 2-mg extracts to reduce nonspecific immunoglobulin binding. After 1 h of incubation, the supernatant was transferred to a new tube. To test the effect of JA on the interaction of MED25 with MYC2, the supernatant was incubated with or without 100 μM methyl jasmonate (MeJA) (Sigma-Aldrich) for 30 min at 4°C before immunoprecipitation of the protein complexes. Myc antibody-bound agarose beads (Santa Cruz) were then added to each reaction for 1 h at 4°C. For negative controls, immunoprecipitation was performed without antibody. The precipitated samples were washed at least four times with the lysis buffer and then eluted by adding 1× SDS protein loading buffer with boiling for 5 min. Co-IP using *35S$_{pro}$:ABI5-4myc* was similar, except that the protein extracts were incubated with or without (±) ABA (Sigma-Aldrich) at 10 μM for 3 h at 4°C before immunoprecipitation of the protein complexes. To test the interaction of MED25 with TPL in plants, 6-d-old *35S$_{pro}$:TPL-GFP* plants were used in Co-IP assays, and 3 mg of protein extracts were precleared with the protein G plus agarose beads and incubated with GFP antibody (Abcam) and the protein G plus agarose beads at 4°C for 4 h.

BiFC Assays

Full-length coding sequences of MED25, MYC2, ABI5, and derivatives of MED25 were cloned into the binary N-terminal fragment of YFP or the C-terminal fragment of YFP vector through Gateway reaction with pENTR vector system (Invitrogen) and sequence verified. Primers for the construction are listed in Supplemental Table 2 online. The resulting constructs were then introduced into *Agrobacterium* strain GV3101. *N. benthamiana* infiltration was performed as described (Song et al., 2011). After infiltration, plants were incubated for at least 50 h before observation. The YFP fluorescence was imaged under a Leica confocal laser scanning microscope (Leica Microsystems). Leaves were infiltrated with 2 μg/mL 4',6-diamidino-2-phenylindole for nuclei staining 2 h before observation.

ChIP-PCR Assays

ChIP assays were performed following a published protocol (Gendrel et al., 2005) with minor modifications. Briefly, 1.5 g of *35S$_{pro}$:MED25-GFP*, *35S$_{pro}$:MED25-4myc*, *35S$_{pro}$:MYC2-GFP*, *35S$_{pro}$:ABI5-4myc*, *35S$_{pro}$:TPL-GFP*, Col-0, or *med25-4* seedlings were cross-linked in 1% formaldehyde and their chromatin isolated. GFP antibody (Abcam), myc antibody (Millipore), or RPB2 antibody (catalog no. ab10338; Abcam) was used to immunoprecipitate the protein-DNA complex, and the precipitated DNA was purified using a PCR purification kit (Qiagen) for qRT-PCR analysis. The ChIP experiments were performed three times. Chromatin precipitated without antibody was used as negative control, while the isolated chromatin before precipitation was used as input control. Primers used for ChIP-PCR are listed in Supplemental Table 3 online.

RNA Extraction and Gene Expression Analyses

For qRT-PCR analysis of JA-responsive genes, total RNA was extracted from 10-d-old seedlings treated with MeJA as indicated (using Trizol [Invitrogen] reagent). For qRT-PCR analysis of ABA-responsive genes, seeds were germinated on 10 μM ABA for 3 d after stratification. Total RNA was extracted using the RNAqueous kit (Ambion) for small-scale RNA isolation. cDNA was prepared from 2 μg of total RNA with Superscript III reverse transcriptase (Invitrogen) and quantified with an cycler apparatus (Roche 480) with the SYBR Green kit (Takara) according to the manufacturer's instructions. Expression levels of target genes were normalized to *ACTIN7*, and the expression levels in Col-0 without hormone treatment were arbitrarily set to 1. The statistical significance was evaluated by Student's *t* test. Primers used for qRT-PCR are listed in Supplemental Table 3 online.

Antibody Generation

Full-length coding sequence of *MED25* was PCR amplified from reverse transcription product with gene-specific primers (see Supplemental Table 2 online). The resulting PCR product was cloned into the *Bam*HI and *Sal*I sites of the pMAL-c2 vector (NEB) to express MBP-MED25 protein in *Escherichia coli* strain BL21. The recombinant fusion protein was purified with amylase resin (NEB) and used to raise polyclonal antibodies in mouse. The antibodies were used in MED25 immunoblots at a final concentration of 1:1000.

Immunoblot Assays

For ABI5 protein level analysis, protein extraction was performed by homogenizing 10-d-old seedlings in extraction buffer (50 mM Tris-HCl, pH 7.5, 100 mM NaCl, 0.1% Nonidet P-40, 10% glycerol, 1 μM DTT, 20 μM MG132, and Roche protease inhibitor cocktail). For immunoblot analysis, SDS sample buffer was added to the protein extracts. Protein samples were boiled for 5 min, separated on SDS-PAGE gels, and transferred to polyvinylidene fluoride membranes. Immunoblots were probed with anti-myc antibody (Abmart). Ponceau S–stained membranes are shown as loading controls.

For MYC2-4myc immunoblots, an anti-myc antibody (Abmart) was used at a final dilution of 1:2000. For TPL-GFP immunoblots, an anti-GFP antibody (Abcam) was used at a final dilution of 1:1000.

Pst DC3000 Infection

Inoculation of *Pst* strain DC3000 was performed as previously described (Liang et al., 2009). To determine bacterial growth, infected leaves were collected at 0 and 3 d after inoculation. At each time point, 10 leaves were collected from each genotype.

Accession Numbers

Sequence data from this article can be found in the Arabidopsis Genome Initiative under the following accession numbers: *MED25* (At1g25540), *ACTIN7* (At5g09810), *MYC2* (At1g32640), *COI1* (At2g39940), *ABI5* (At2g36270), *JAZ1* (At1g19180), *JAZ2* (At1g74950), *JAZ3* (At3g17860), *JAZ5* (At1g17380), *JAZ6* (At1g72450), *JAZ7* (At2g34600), *JAZ8* (At1g30135), *JAZ9* (At1g70700), *JAZ10* (At5g13220), *JAZ12* (At5g20900), *VSP1* (At5g24780), *PDF1.2* (At5g44420), *ERF1* (At3g23240), *LOX2* (At3g45140), *Em1* (At3g51810), *Em6* (At2g40170), *RAB18* (At5g66400), *TPL* (At1g15750), *NINJA* (At4g28910), and *NRPB2* (At4g21710).

Supplemental Data

The following materials are available in the online version of this article.

Supplemental Figure 1. Genetic Complementation of the *ber6*/*med25-4* Mutant.

Supplemental Figure 2. qRT-PCR Analyses of JA-Induced Expression of the *JAZ* Family Genes in Col-0 and *med25-4*.

Supplemental Figure 3. Yeast Assays Showing That the Transcriptional Activity of MED25 Can Be Suppressed by 3-AT.

Supplemental Figure 4. Yeast Two-Hybrid Assays with MED25, NINJA, and TPL.

Supplemental Figure 5. MED25 Negatively Regulates the Function of ABI5 in ABA Signaling.

Supplemental Table 1. DNA Primers Used for Map-Based Cloning and Diagnostic PCR.

Supplemental Table 2. DNA Primers Used for Construct Generation.

Supplemental Table 3. DNA Primers Used for qRT-PCR and ChIP-qPCR Assays.

ACKNOWLEDGMENTS

We thank Joanne Chory and Daoxin Xie for sharing their research materials with us. This work was supported by the Ministry of Agriculture of China (2011ZX08009-003-001), The Ministry of Science and Technology of China (2011CB915400), the National Natural Science Foundation of China (31030006, 91117013, and 31070251), and the State Key Laboratory of Plant Genomics of China (2011B0525-02).

AUTHOR CONTRIBUTIONS

R.C. and H.J. designed and performed the research, analyzed the data, and wrote the article. L.L., Q.Z., L.Q., W.Z., X.L. H.L., W.Z., and J.S. performed the research and analyzed the data. C.L. supervised and designed the research, analyzed the data, and wrote the article.

Received March 15, 2012; revised June 21, 2012; accepted July 2, 2012; published July 20, 2012.

REFERENCES

Abe, H., Urao, T., Ito, T., Seki, M., Shinozaki, K., and Yamaguchi-Shinozaki, K. (2003). *Arabidopsis* AtMYC2 (bHLH) and AtMYB2 (MYB) function as transcriptional activators in abscisic acid signaling. Plant Cell **15:** 63–78.

Adie, B.A., Pérez-Pérez, J., Pérez-Pérez, M.M., Godoy, M., Sánchez-Serrano, J.J., Schmelz, E.A., and Solano, R. (2007). ABA is an essential signal for plant resistance to pathogens affecting JA biosynthesis and the activation of defenses in *Arabidopsis*. Plant Cell **19:** 1665–1681.

Anderson, J.P., Badruzsaufari, E., Schenk, P.M., Manners, J.M., Desmond, O.J., Ehlert, C., Maclean, D.J., Ebert, P.R., and Kazan, K. (2004). Antagonistic interaction between abscisic acid and jasmonate-ethylene signaling pathways modulates defense gene expression and disease resistance in *Arabidopsis*. Plant Cell **16:** 3460–3479.

Autran, D., Jonak, C., Belcram, K., Beemster, G.T., Kronenberger, J., Grandjean, O., Inzé, D., and Traas, J. (2002). Cell numbers and leaf development in *Arabidopsis*: A functional analysis of the *STRUWWELPETER* gene. EMBO J. **21:** 6036–6049.

Bäckström, S., Elfving, N., Nilsson, R., Wingsle, G., and Björklund, S. (2007). Purification of a plant mediator from *Arabidopsis thaliana* identifies PFT1 as the Med25 subunit. Mol. Cell **26:** 717–729.

Bensmihen, S., Rippa, S., Lambert, G., Jublot, D., Pautot, V., Granier, F., Giraudat, J., and Parcy, F. (2002). The homologous ABI5 and EEL transcription factors function antagonistically to fine-tune gene expression during late embryogenesis. Plant Cell **14:** 1391–1403.

Berger, S., Bell, E., and Mullet, J.E. (1996). Two methyl jasmonate-insensitive mutants show altered expression of *AtVsp* in response to methyl jasmonate and wounding. Plant Physiol. **111:** 525–531.

Berger, S., Bell, E., Sadka, A., and Mullet, J.E. (1995). *Arabidopsis thaliana* Atvsp is homologous to soybean VspA and VspB, genes encoding vegetative storage protein acid phosphatases, and is regulated similarly by methyl jasmonate, wounding, sugars, light and phosphate. Plant Mol. Biol. **27:** 933–942.

Bharti, K., Schmidt, E., Lyck, R., Heerklotz, D., Bublak, D., and Scharf, K.D. (2000). Isolation and characterization of HsfA3, a new heat stress transcription factor of *Lycopersicon peruvianum*. Plant J. **22:** 355–365.

Borggrefe, T., and Yue, X. (2011). Interactions between subunits of the Mediator complex with gene-specific transcription factors. Semin. Cell Dev. Biol. **22:** 759–768.

Boter, M., Ruíz-Rivero, O., Abdeen, A., and Prat, S. (2004). Conserved MYC transcription factors play a key role in jasmonate signaling both in tomato and *Arabidopsis*. Genes Dev. **18:** 1577–1591.

Browse, J. (2005). Jasmonate: An oxylipin signal with many roles in plants. Vitam. Horm. **72:** 431–456.

Browse, J. (2009). Jasmonate passes muster: A receptor and targets for the defense hormone. Annu. Rev. Plant Biol. **60:** 183–205.

Bu, Q., Li, H., Zhao, Q., Jiang, H., Zhai, Q., Zhang, J., Wu, X., Sun, J., Xie, Q., Wang, D., and Li, C. (2009). The *Arabidopsis* RING finger E3 ligase RHA2a is a novel positive regulator of abscisic acid signaling during seed germination and early seedling development. Plant Physiol. **150:** 463–481.

Carles, C., Bies-Etheve, N., Aspart, L., Léon-Kloosterziel, K.M., Koornneef, M., Echeverria, M., and Delseny, M. (2002). Regulation of *Arabidopsis thaliana Em* genes: Role of ABI5. Plant J. **30:** 373–383.

Cerdán, P.D., and Chory, J. (2003). Regulation of flowering time by light quality. Nature **423:** 881–885.

Chadick, J.Z., and Asturias, F.J. (2005). Structure of eukaryotic Mediator complexes. Trends Biochem. Sci. **30:** 264–271.

Chen, Q., et al. (2011). The basic helix-loop-helix transcription factor MYC2 directly represses PLETHORA expression during jasmonate-mediated modulation of the root stem cell niche in *Arabidopsis*. Plant Cell **23:** 3335–3352.

Chen, W., and Roeder, R.G. (2011). Mediator-dependent nuclear receptor function. Semin. Cell Dev. Biol. **22:** 749–758.

Chini, A., Fonseca, S., Fernández, G., Adie, B., Chico, J.M., Lorenzo, O., García-Casado, G., López-Vidriero, I., Lozano, F.M., Ponce, M.R., Micol, J.L., and Solano, R. (2007). The JAZ family of repressors is the missing link in jasmonate signalling. Nature **448:** 666–671.

Chung, H.S., Niu, Y., Browse, J., and Howe, G.A. (2009). Top hits in contemporary JAZ: An update on jasmonate signaling. Phytochemistry **70:** 1547–1559.

Conaway, R.C., and Conaway, J.W. (2011). Function and regulation of the Mediator complex. Curr. Opin. Genet. Dev. **21:** 225–230.

Creelman, R.A., and Mullet, J.E. (1997). Oligosaccharins, brassinolides, and jasmonates: Nontraditional regulators of plant growth, development, and gene expression. Plant Cell **9:** 1211–1223.

Dombrecht, B., Xue, G.P., Sprague, S.J., Kirkegaard, J.A., Ross, J.J., Reid, J.B., Fitt, G.P., Sewelam, N., Schenk, P.M., Manners, J.M., and Kazan, K. (2007). MYC2 differentially modulates diverse jasmonate-dependent functions in *Arabidopsis*. Plant Cell **19:** 2225–2245.

Elfving, N., Davoine, C., Benlloch, R., Blomberg, J., Brännström, K., Müller, D., Nilsson, A., Ulfstedt, M., Ronne, H., Wingsle, G., Nilsson, O., and Björklund, S. (2011). The *Arabidopsis thaliana* Med25 mediator subunit integrates environmental cues to control plant development. Proc. Natl. Acad. Sci. USA **108:** 8245–8250.

Ellis, C., and Turner, J.G. (2002). A conditionally fertile *coi1* allele indicates cross-talk between plant hormone signalling pathways in *Arabidopsis thaliana* seeds and young seedlings. Planta **215:** 549–556.

Fernández-Arbaizar, A., Regalado, J.J., and Lorenzo, O. (2012). Isolation and characterization of novel mutant loci suppressing the ABA hypersensitivity of the *Arabidopsis coronatine insensitive 1-16* (*coi1-16*) mutant during germination and seedling growth. Plant Cell Physiol. **53:** 53–63.

Fernández-Calvo, P., et al. (2011). The *Arabidopsis* bHLH transcription factors MYC3 and MYC4 are targets of JAZ repressors and act additively with MYC2 in the activation of jasmonate responses. Plant Cell **23:** 701–715.

Flanagan, P.M., Kelleher, R.J., IIISayre, M.H., Tschochner, H., and Kornberg, R.D. (1991). A mediator required for activation of RNA polymerase II transcription in vitro. Nature **350:** 436–438.

Fonseca, S., Chini, A., Hamberg, M., Adie, B., Porzel, A., Kramell, R., Miersch, O., Wasternack, C., and Solano, R. (2009). (+)-7-iso-Jasmonoyl-L-isoleucine is the endogenous bioactive jasmonate. Nat. Chem. Biol. **5:** 344–350.

Fujita, Y., Fujita, M., Shinozaki, K., and Yamaguchi-Shinozaki, K. (2011). ABA-mediated transcriptional regulation in response to osmotic stress in plants. J. Plant Res. **124:** 509–525.

Gendrel, A.V., Lippman, Z., Martienssen, R., and Colot, V. (2005). Profiling histone modification patterns in plants using genomic tiling microarrays. Nat. Methods **2:** 213–218.

Gillmor, C.S., Park, M.Y., Smith, M.R., Pepitone, R., Kerstetter, R. A., and Poethig, R.S. (2010). The MED12-MED13 module of Mediator regulates the timing of embryo patterning in *Arabidopsis*. Development **137:** 113–122.

Hentges, K.E. (2011). Mediator complex proteins are required for diverse developmental processes. Semin. Cell Dev. Biol. **22:** 769–775.

Hou, X., Lee, L.Y., Xia, K., Yan, Y., and Yu, H. (2010). DELLAs modulate jasmonate signaling via competitive binding to JAZs. Dev. Cell **19:** 884–894.

Howe, G.A., and Jander, G. (2008). Plant immunity to insect herbivores. Annu. Rev. Plant Biol. **59:** 41–66.

Ito, J., Sono, T., Tasaka, M., and Furutani, M. (2011). MACCHI-BOU 2 is required for early embryo patterning and cotyledon organogenesis in *Arabidopsis*. Plant Cell Physiol. **52:** 539–552.

Katsir, L., Chung, H.S., Koo, A.J., and Howe, G.A. (2008). Jasmonate signaling: A conserved mechanism of hormone sensing. Curr. Opin. Plant Biol. **11:** 428–435.

Kazan, K., and Manners, J.M. (2008). Jasmonate signaling: Toward an integrated view. Plant Physiol. **146:** 1459–1468.

Kelleher, R.J., IIIFlanagan, P.M., and Kornberg, R.D. (1990). A novel mediator between activator proteins and the RNA polymerase II transcription apparatus. Cell **61:** 1209–1215.

Kidd, B.N., Aitken, E.A., Schenk, P.M., Manners, J.M., and Kazan, K. (2010). Plant mediator: Mediating the jasmonate response. Plant Signal. Behav. **5:** 718–720.

Kidd, B.N., Cahill, D.M., Manners, J.M., Schenk, P.M., and Kazan, K. (2011). Diverse roles of the Mediator complex in plants. Semin. Cell Dev. Biol. **22:** 741–748.

Kidd, B.N., Edgar, C.I., Kumar, K.K., Aitken, E.A., Schenk, P.M., Manners, J.M., and Kazan, K. (2009). The mediator complex subunit PFT1 is a key regulator of jasmonate-dependent defense in *Arabidopsis*. Plant Cell **21:** 2237–2252.

Kim, Y.J., and Chen, X. (2011). The plant Mediator and its role in noncoding RNA production. Front. Biol. **6:** 125–132.

Kim, Y.J., Zheng, B., Yu, Y., Won, S.Y., Mo, B., and Chen, X. (2011). The role of Mediator in small and long noncoding RNA production in *Arabidopsis thaliana*. EMBO J. **30:** 814–822.

Kloek, A.P., Verbsky, M.L., Sharma, S.B., Schoelz, J.E., Vogel, J., Klessig, D.F., and Kunkel, B.N. (2001). Resistance to *Pseudomonas syringae* conferred by an *Arabidopsis thaliana* coronatine-insensitive (*coi1*) mutation occurs through two distinct mechanisms. Plant J. **26:** 509–522.

Lång, V., and Palva, E.T. (1992). The expression of a rab-related gene, *rab18*, is induced by abscisic acid during the cold acclimation process of *Arabidopsis thaliana (L.) Heynh*. Plant Mol. Biol. **20:** 951–962.

Larivière, L., Seizl, M., and Cramer, P. (2012). A structural perspective on Mediator function. Curr. Opin. Cell Biol. **24:** 305–313.

Laurie-Berry, N., Joardar, V., Street, I.H., and Kunkel, B.N. (2006). The *Arabidopsis thaliana* JASMONATE INSENSITIVE 1 gene is required for suppression of salicylic acid-dependent defenses during infection by *Pseudomonas syringae*. Mol. Plant Microbe Interact. **19:** 789–800.

Lee, H.K., Park, U.H., Kim, E.J., and Um, S.J. (2007). MED25 is distinct from TRAP220/MED1 in cooperating with CBP for retinoid receptor activation. EMBO J. **26:** 3545–3557.

Li, H., Jiang, H., Bu, Q., Zhao, Q., Sun, J., Xie, Q., and Li, C. (2011). The *Arabidopsis* RING finger E3 ligase RHA2b acts additively with RHA2a in regulating abscisic acid signaling and drought response. Plant Physiol. **156:** 550–563.

Liang, W., Li, C., Liu, F., Jiang, H., Li, S., Sun, J., Wu, X., and Li, C. (2009). The *Arabidopsis* homologs of CCR4-associated factor 1 show mRNA deadenylation activity and play a role in plant defence responses. Cell Res. **19:** 307–316.

Lopez-Molina, L., Mongrand, S., and Chua, N.H. (2001). A post-germination developmental arrest checkpoint is mediated by abscisic acid and requires the ABI5 transcription factor in *Arabidopsis*. Proc. Natl. Acad. Sci. USA **98:** 4782–4787.

Lopez-Molina, L., Mongrand, S., Kinoshita, N., and Chua, N.H. (2003). AFP is a novel negative regulator of ABA signaling that promotes ABI5 protein degradation. Genes Dev. **17:** 410–418.

Lopez-Molina, L., Mongrand, S., McLachlin, D.T., Chait, B.T., and Chua, N.H. (2002). ABI5 acts downstream of ABI3 to execute an ABA-dependent growth arrest during germination. Plant J. **32:** 317–328.

Lorenzo, O., Chico, J.M., Sánchez-Serrano, J.J., and Solano, R. (2004). JASMONATE-INSENSITIVE1 encodes a MYC transcription factor essential to discriminate between different jasmonate-regulated defense responses in *Arabidopsis*. Plant Cell **16:** 1938–1950.

Malik, S., and Roeder, R.G. (2005). Dynamic regulation of pol II transcription by the mammalian Mediator complex. Trends Biochem. Sci. **30:** 256–263.

Malik, S., and Roeder, R.G. (2010). The metazoan Mediator co-activator complex as an integrative hub for transcriptional regulation. Nat. Rev. Genet. **11:** 761–772.

Mittler, G., Stühler, T., Santolin, L., Uhlmann, T., Kremmer, E., Lottspeich, F., Berti, L., and Meisterernst, M. (2003). A novel docking site on Mediator is critical for activation by VP16 in mammalian cells. EMBO J. **22:** 6494–6504.

Mockaitis, K., and Estelle, M. (2008). Auxin receptors and plant development: A new signaling paradigm. Annu. Rev. Cell Dev. Biol. **24:** 55–80.

Nakamura, S., Lynch, T.J., and Finkelstein, R.R. (2001). Physical interactions between ABA response loci of *Arabidopsis*. Plant J. **26:** 627–635.

Nakamura, Y., et al. (2011). Wwp2 is essential for palatogenesis mediated by the interaction between Sox9 and mediator subunit 25. Nat. Commun. **2:** 251.

Nambara, E., Suzuki, M., Abrams, S., McCarty, D.R., Kamiya, Y., and McCourt, P. (2002). A screen for genes that function in abscisic acid signaling in *Arabidopsis thaliana*. Genetics **161:** 1247–1255.

Onodera, Y., Haag, J.R., Ream, T., Costa Nunes, P., Pontes, O., and Pikaard, C.S. (2005). Plant nuclear RNA polymerase IV mediates siRNA and DNA methylation-dependent heterochromatin formation. Cell **120:** 613–622.

Onodera, Y., Nakagawa, K., Haag, J.R., Pikaard, D., Mikami, T., Ream, T., Ito, Y., and Pikaard, C.S. (2008). Sex-biased lethality or transmission of defective transcription machinery in Arabidopsis. Genetics **180:** 207–218.

Ou, B., Yin, K.Q., Liu, S.N., Yang, Y., Gu, T., Wing Hui, J.M., Zhang, L., Miao, J., Kondou, Y., Matsui, M., Gu, H.Y., and Qu, L.J. (2011). A high-throughput screening system for *Arabidopsis* transcription factors and its application to Med25-dependent transcriptional regulation. Mol. Plant **4:** 546–555.

Pauwels, L., et al. (2010). NINJA connects the co-repressor TOPLESS to jasmonate signalling. Nature **464:** 788–791.

Pauwels, L., Inzé, D., and Goossens, A. (2009). Jasmonate-inducible gene: What does it mean? Trends Plant Sci. **14:** 87–91.

Penninckx, I.A., Eggermont, K., Terras, F.R., Thomma, B.P., De Samblanx, G.W., Buchala, A., Métraux, J.P., Manners, J.M., and Broekaert, W.F. (1996). Pathogen-induced systemic activation of a plant defensin gene in *Arabidopsis* follows a salicylic acid-independent pathway. Plant Cell **8:** 2309–2323.

Qi, T., Song, S., Ren, Q., Wu, D., Huang, H., Chen, Y., Fan, M., Peng, W., Ren, C., and Xie, D. (2011). The Jasmonate-ZIM-domain proteins interact with the WD-Repeat/bHLH/MYB complexes to regulate Jasmonate-mediated anthocyanin accumulation and trichome initiation in *Arabidopsis thaliana*. Plant Cell **23:** 1795–1814.

Rana, R., Surapureddi, S., Kam, W., Ferguson, S., and Goldstein, J.A. (2011). Med25 is required for RNA polymerase II recruitment to specific promoters, thus regulating xenobiotic and lipid metabolism in human liver. Mol. Cell. Biol. **31:** 466–481.

Ries, D., and Meisterernst, M. (2011). Control of gene transcription by Mediator in chromatin. Semin. Cell Dev. Biol. **22:** 735–740.

Robson, F., Okamoto, H., Patrick, E., Harris, S.R., Wasternack, C., Brearley, C., and Turner, J.G. (2010). Jasmonate and phytochrome A signaling in *Arabidopsis* wound and shade responses are integrated through JAZ1 stability. Plant Cell **22:** 1143–1160.

Sharma, D., and Fondell, J.D. (2002). Ordered recruitment of histone acetyltransferases and the TRAP/Mediator complex to thyroid hormone-responsive promoters in vivo. Proc. Natl. Acad. Sci. USA **99:** 7934–7939.

Sheard, L.B., et al. (2010). Jasmonate perception by inositol-phosphate-potentiated COI1-JAZ co-receptor. Nature **468:** 400–405.

Song, S., Qi, T., Huang, H., Ren, Q., Wu, D., Chang, C., Peng, W., Liu, Y., Peng, J., and Xie, D. (2011). The Jasmonate-ZIM domain proteins interact with the R2R3-MYB transcription factors MYB21 and MYB24 to affect Jasmonate-regulated stamen development in *Arabidopsis*. Plant Cell **23:** 1000–1013.

Spoel, S.H., Mou, Z., Tada, Y., Spivey, N.W., Genschik, P., and Dong, X. (2009). Proteasome-mediated turnover of the transcription coactivator NPR1 plays dual roles in regulating plant immunity. Cell **137:** 860–872.

Staswick, P.E., Su, W., and Howell, S.H. (1992). Methyl jasmonate inhibition of root growth and induction of a leaf protein are decreased in an *Arabidopsis thaliana* mutant. Proc. Natl. Acad. Sci. USA **89:** 6837–6840.

Staswick, P.E., and Tiryaki, I. (2004). The oxylipin signal jasmonic acid is activated by an enzyme that conjugates it to isoleucine in *Arabidopsis*. Plant Cell **16:** 2117–2127.

Stone, S.L., Williams, L.A., Farmer, L.M., Vierstra, R.D., and Callis, J. (2006). KEEP ON GOING, a RING E3 ligase essential for *Arabidopsis* growth and development, is involved in abscisic acid signaling. Plant Cell **18:** 3415–3428.

Sun, J.Q., Jiang, H.L., and Li, C.Y. (2011). Systemin/Jasmonate-mediated systemic defense signaling in tomato. Mol. Plant **4:** 607–615.

Sun, J., et al. (2009). *Arabidopsis ASA1* is important for jasmonate-mediated regulation of auxin biosynthesis and transport during lateral root formation. Plant Cell **21:** 1495–1511.

Suza, W.P., Rowe, M.L., Hamberg, M., and Staswick, P.E. (2010). A tomato enzyme synthesizes (+)-7-iso-jasmonoyl-L-isoleucine in wounded leaves. Planta **231:** 717–728.

Szemenyei, H., Hannon, M., and Long, J.A. (2008). TOPLESS mediates auxin-dependent transcriptional repression during Arabidopsis embryogenesis. Science **319:** 1384–1386.

Tamura, N., Yoshida, T., Tanaka, A., Sasaki, R., Bando, A., Toh, S., Lepiniec, L., and Kawakami, N. (2006). Isolation and characterization of high temperature-resistant germination mutants of *Arabidopsis thaliana*. Plant Cell Physiol. **47:** 1081–1094.

Thines, B., Katsir, L., Melotto, M., Niu, Y., Mandaokar, A., Liu, G., Nomura, K., He, S.Y., Howe, G.A., and Browse, J. (2007). JAZ repressor proteins are targets of the SCF(COI1) complex during jasmonate signalling. Nature **448:** 661–665.

Turner, J.G., Ellis, C., and Devoto, A. (2002). The jasmonate signal pathway. Plant Cell **14** (suppl.)**:** S153–S164.

Wang, W., and Chen, X. (2004). HUA ENHANCER3 reveals a role for a cyclin-dependent protein kinase in the specification of floral organ identity in *Arabidopsis*. Development **131:** 3147–3156.

Wasternack, C. (2007). Jasmonates: An update on biosynthesis, signal transduction and action in plant stress response, growth and development. Ann. Bot. (Lond.) **100:** 681–697.

Wasternack, C., and Kombrink, E. (2010). Jasmonates: Structural requirements for lipid-derived signals active in plant stress responses and development. ACS Chem. Biol. **5:** 63–77.

Weinthal, D., and Tzfira, T. (2009). Imaging protein-protein interactions in plant cells by bimolecular fluorescence complementation assay. Trends Plant Sci. **14:** 59–63.

Xie, D.X., Feys, B.F., James, S., Nieto-Rostro, M., and Turner, J.G. (1998). COI1: An *Arabidopsis* gene required for jasmonate-regulated defense and fertility. Science **280:** 1091–1094.

Xu, L., Liu, F., Lechner, E., Genschik, P., Crosby, W.L., Ma, H., Peng, W., Huang, D., and Xie, D. (2002). The SCF(^{COI1}) ubiquitin-ligase complexes are required for jasmonate response in *Arabidopsis*. Plant Cell **14:** 1919–1935.

Xu, R., and Li, Y. (2011). Control of final organ size by Mediator complex subunit 25 in *Arabidopsis thaliana*. Development **138:** 4545–4554.

Yan, J., Zhang, C., Gu, M., Bai, Z., Zhang, W., Qi, T., Cheng, Z., Peng, W., Luo, H., Nan, F., Wang, Z., and Xie, D. (2009). The *Arabidopsis* CORONATINE INSENSITIVE1 protein is a jasmonate receptor. Plant Cell **21:** 2220–2236.

Yan, Y., Stolz, S., Chételat, A., Reymond, P., Pagni, M., Dubugnon, L., and Farmer, E.E. (2007). A downstream mediator in the growth repression limb of the jasmonate pathway. Plant Cell **19:** 2470–2483.

Yang, F., DeBeaumont, R., Zhou, S., and Näär, A.M. (2004). The activator-recruited cofactor/Mediator coactivator subunit ARC92 is a functionally important target of the VP16 transcriptional activator. Proc. Natl. Acad. Sci. USA **101:** 2339–2344.

Zarei, A., Körbes, A.P., Younessi, P., Montiel, G., Champion, A., and Memelink, J. (2011). Two GCC boxes and AP2/ERF-domain transcription factor ORA59 in jasmonate/ethylene-mediated activation of the *PDF1.2* promoter in *Arabidopsis*. Plant Mol. Biol. **75:** 321–331.

Zheng, B., Wang, Z., Li, S., Yu, B., Liu, J.Y., and Chen, X. (2009). Intergenic transcription by RNA polymerase II coordinates Pol IV and Pol V in siRNA-directed transcriptional gene silencing in Arabidopsis. Genes Dev. **23:** 2850–2860.

Zheng, W., Zhai, Q., Sun, J., Li, C.B., Zhang, L., Li, H., Zhang, X., Li, S., Xu, Y., Jiang, H., Wu, X., and Li, C. (2006). Bestatin, an inhibitor of aminopeptidases, provides a chemical genetics approach to dissect jasmonate signaling in Arabidopsis. Plant Physiol. **141:** 1400–1413.

Zhu, Z., et al. (2011). Derepression of ethylene-stabilized transcription factors (EIN3/EIL1) mediates jasmonate and ethylene signaling synergy in *Arabidopsis*. Proc. Natl. Acad. Sci. USA **108:** 12539–12544.